# Dimensioning of a hydrogen storage system

*Duarte Pinto Magalhães*

**Master Dissertation**

Supervisor at FEUP: Prof. Adélio Cavadas




**Masters in Fluids and Energy**

2022-09-26

# Abstract

The present work deals with the concession of a charging system for the storage of hydrogen gas in macro-spheres, patented by Stenmark. The main objective is to study and conceptualize a charging system, taking into account the most suitable materials for working with hydrogen, as well as the components of charging systems that are most commonly used in this type of applications.

Throughout the dissertation it was sought to study: (1) the description of hydrogen as an energy vector; (2) the storage of energy in the form of compressed hydrogen, cryogenic liquid and also as metal hydride; (3) the storage of gaseous hydrogen in macro-spheres, as well as its advantages and disadvantages compared to other existing gaseous hydrogen storage methods; (4) the hydrogen permeation phenomenon; (5) the study of hydrogen compatible materials; (6) the study of charging system components such as compressors and valves that can be used for the application.

After obtaining the results it is possible to state that, for the chosen charging system model, the tanks should be charged to a pressure of 1000 *bar* at an approximately constant temperature of 37 $^{\circ}C$. Knowing that the proposed volume for two types of tanks is 699 and 472 *l*, the charging time for these tanks will be 99 and 67 minutes, respectively. To compress one kilogram of hydrogen to a pressure of 1000 *bar*, at least 17937.83 *kJ* of energy is spent, which represents 14% of the potential energy that can be extracted from one kilogram of hydrogen. The charging system presents pipelines made of 316L stainless steel, which in addition to having good mechanical properties, is very resistant to corrosion caused by hydrogen. After studying the pressure losses along 5 *m* of duct, it was possible to conclude that for a duct with an inner diameter of 8 *mm* about 2156 *Pa* are lost, a value that is approximately 20 times higher than the pressure lost for a duct with inner diameter of 17 *mm*, with the same length, which implies that the smaller duct diameter is not suitable for the application under study.

After the completion of this work, it was possible to conclude that the use of hydrogen as an energy vector is a viable alternative, since, from an environmental point of view, it unquestionably offers benefits, mainly due to its low pollutant emissions, depending on the pollutant and oxidizer. However, handling compressed hydrogen at high pressures will always raise safety concerns due to the explosive characteristics of the gas. Additionally, to store energy in the form of compressed hydrogen, a significant amount of the potential energy of the gas is wasted, making the option less efficient.

**Keywords**: Hydrogen; Hydrogen Storage; Charging System; Energy Efficiency; Pressure Loss.

# Resumo

O presente trabalho aborda a concessão de um sistema de enchimento para o armazenamento de hidrogénio gasoso em macro-esferas, patenteado por Stenmark. O principal objetivo é estudar e concetualizar um sistema de enchimento, tendo em conta os materiais mais adequados para o trabalho com o hidrogénio, como também os componentes de sistemas de enchimento que são mais utilizados neste tipo de aplicações.

Ao longo da realização desta dissertação procorou-se estudar: (1) a descrição do hidrogénio como vetor energético; (2) o armazenamento de energia sob a forma de hidrogénio comprimido, líquido criogénico e também como hidreto de metal; (3) o armazenamento de hidrogénio gasoso em macro-esferas, assim como as suas vantagens e desvantagens perante outros métodos de armazenamento em hidrogénio gasoso já existentes; (4) o fenómeno de permeação do hidrogénio; (5) o estudo de materiais compatíveis com o hidrogénio; (6) o estudo de componentes de sistemas de enchimento, como compressores e válvulas que podem ser utilizados para a aplicação.

Após a obtenção dos resultados é possível afirmar que, para o modelo de sistema de enchimento escolhido, os tanques deverão ser carregados até à pressão de 1000 *bar* a uma temperatura aproximadamente constante de 37 $°C$. Sabendo que o volume proposto para dois tipos de tanques é de 699 e 472 $l$, o tempo de enchimento destes irá ser 99 e 67 minutos, respetivamente. Para a compressão de um quilograma de hidrogénio até à pressão de 1000 *bar* são gastos, no mínimo, 17937.83 $kJ$ de energia, valor que representa 14% da energia potencial que pode ser extraída de um quilograma de hidrogénio. O sistema de enchimento apresenta condutas de um aço inoxidável 316L, que para além de apresentar boas propriedades mecânicas, é bastante resistente à corrosão provocada pelo hidrogénio. Após o estudo das perdas de pressão ao longo de 5 $m$ de conduta, foi possível concluir que para uma conduta com um diâmetro interior de 8 *mm* são perdidos cerca de 2156 *Pa*, valor que é aproximadamente 20 vezes maior do que o valor de pressão perdida para uma conduta de 17 *mm* de diâmetro interior, com o mesmo comprimento, o que implica que o menor diâmetro de conduta não se adequa para a aplicação em estudo.

Após a conclusão deste trabalho, foi possível concluir que a utilização do hidrogénio como vetor energético é uma alternativa viável, uma vez que, do ponto de vista ambiental, oferece inquestionavelmente benefícios, principalmente devido às suas baixas emissões poluentes. No entanto, o manuseamento do hidrogénio comprimido a pressões elevadas suscitará sempre preocupações de segurança devido às características explosivas do gás. Adicionalmente, para armazenar energia sob a forma de hidrogénio comprimido, uma quantidade significativa do potencial energético do gás é desperdiçada, tornando a opção menos eficiente.

**Palavras-chave**: Hidrogénio; Armazenamento de Hidrogénio; Sistema de Carregamento; Eficiência Energética; Perda de Pressão.

# Acknowledgments

I would like to thank all my friends and family, who supported me throughout this journey. I will be forever thankful for all the advice and guidance that they provided, as well as moral support. I would like to give a special thank you to professor Adélio Cavadas and professor Leonardo Ribeiro for being present and available during the realization of this dissertation.

# Contents


**1 Introduction** **1**
- 1.1 Project contextualization and motivation . . . 1
- 1.2 Objectives . . . 1
- 1.3 Methodology . . . 1
- 1.4 Structure of the dissertation . . . 2

**2 Literature review** **3**
- 2.1 Hydrogen . . . 3
- 2.2 Hydrogen Storage . . . 3
  - 2.2.1 Compressed gas storage . . . 4
  - 2.2.2 Cryogenic liquid storage . . . 5
  - 2.2.3 Reverse metal hydride storage . . . 6
  - 2.2.4 Other methods . . . 7
- 2.3 Spheres storage method . . . 7
  - 2.3.1 Components . . . 9

**3 Problem Description** **19**
- 3.1 Tank Dimensions . . . 19
- 3.2 Charging/discharging methods . . . 20
- 3.3 Adopted spheres charging method . . . 25

**4 Methodology** **27**
- 4.1 Hydrogen piping design . . . 27
  - 4.1.1 Piping design . . . 27
  - 4.1.2 Pressure loss . . . 31

**5 Results** **35**
- 5.1 Hydrogen piping . . . 35
  - 5.1.1 Hydrogen compressor . . . 35
  - 5.1.2 Piping design . . . 37
  - 5.1.3 Pressure loss . . . 38
- 5.2 Compressed air usage . . . 42
- 5.3 Results Analysis . . . 42

**6 Conclusions and Future Work** **43**
- 6.1 Conclusions . . . 43
- 6.2 Future Work . . . 44

**A Hydrogen Density** **47**

**B 316L Stainless Steel properties** **49**

**C Steel tube profile specifications** **51**

**D K values of different accessories** **53**

# Acronyms and Symbols

## Acronyms

| | |
|---|---|
| GED | Gravimetric Energy Density |
| LH2 | Liquid Hydrogen |
| NTP | Normal Temperature and Pressure |
| VED | Volumetric Energy Density |

## Latin Symbols

| | |
|---|---|
| a | Inside Radius |
| b | Outside Radius |
| D | Diameter |
| E | Young Modulus |
| $E_{comp}$ | Compression Energy |
| f | Darcy Coefficient |
| $h_L$ | Head Loss |
| K | Adimensional Parameter Characteristic of Pipeline Accesories |
| L | Length |
| M | Metal |
| $\dot{m}$ | Mass Flow Rate |
| p | Pressure |
| Pot | Power |
| Q | Volumetric Flow Rate |
| r | Radius |
| Re | Reynolds Number |
| V | Mean Velocity |

## Greek Symbols

| | |
|---|---|
| $\varepsilon$ | Roughness |
| $\rho$ | Density |
| $\sigma_1$ | Normal Stress |
| $\sigma_3$ | Normal Stress |
| $\sigma_e$ | Equivalent Stress |
| $\sigma_l$ | Axial Stress |
| $\sigma_r$ | Radial Stress |
| $\sigma_t$ | Circumferential Stress |
| $\sigma_y$ | Normal Stress (y-axis) |

# List of Figures


2.1 Comparison between the GED and VED for compressed hydrogen gas, cryogenic hydrogen, and other fuels. . . . 4
2.2 Proposed storage system. . . . 7
2.3 On the left, GED and, on the right, weight comparisons. . . . 8
2.4 On the left, VED and, on the right, Stored Hydrogen Mass. . . . 9
2.5 Discharge pressure vs Compressor's capacity. . . . 13
2.6 Schematic of a single-acting reciprocating piston hydrogen compressor. . . . 13
2.7 Schematic of a diaphragm compressor. . . . 14
2.8 Typical one-piece body cast swing disc non-return valve. . . . 15
2.9 Typical closed piston non-return valve. . . . 16
2.10 Butterfly valve. . . . 16
2.11 Lined single-seat globe valve. . . . 17

3.1 Tank 1 swap procedure . . . 19
3.2 Tank 2 swap procedure . . . 20
3.3 Water A1 solution - first step . . . 21
3.4 Water A1 solution - second step . . . 21
3.5 Water A1 solution - third step . . . 22
3.6 Water A1 solution - fourth step . . . 22
3.7 Water A2 solution - first step . . . 23
3.8 Water A2 solution - second step . . . 23
3.9 Water A2 solution - third step . . . 24
3.10 Compressed air solution - first step . . . 24
3.11 Compressed air solution - second step . . . 25
3.12 Compressed air solution - third step . . . 25
3.13 Pressure comparison between the interior and exterior of the spheres . . . 26

4.1 Thick cylinder, inner radius a and exterior radius b. . . . 28
4.2 Stress distribution for a thick cylinder under internal pressure. . . . 29
4.3 Moody Diagram. . . . 32

5.1 Booster example. . . . 35
5.2 Compressor unit with the three boosters. . . . 36
5.3 Illustration of the container with two compressor units. . . . 37
5.4 Proposed second water charging technique . . . 40
5.5 Proposed piping system configuration. . . . 41

A.1 Hydrogen density values at different temperatures and pressures. . . . 47
A.2 Hydrogen density variation at different temperatures and pressures. . . . 48

B.1 316L stainless steel chemical composition. . . . . 49
B.2 316L stainless steel properties. . . . . 49
B.3 316L stainless steel mechanical properties. . . . . 50

C.1 316L stainless steel profile information. . . . . 51

D.1 Accessories K values for local pressure calculation. . . . . 53

# List of Tables


2.1 Working Temperature Limit of some common plastics. . . . . 11
2.2 Permeation Values of some Elastomers. . . . . 12

3.1 Dimensions, Number of spheres, Mass of hydrogen of each type of tank . . . . . 20

5.1 Maximum inner diameter (and thickness) that satisfy the Tresca and Von Mises Criteria . . . . . 38
5.2 Possible outside diameters and corresponding maximum inside diameters of the pipeline . . . . . 38
5.3 Pressure loss values (Pa) depending on pipeline length and interior diameter . . . 39
5.3 Pressure loss values (Pa) depending on pipeline length and interior diameter . . . 40
5.4 Local pressure loss in different equipment . . . . . 41

# Chapter 1

# Introduction

## 1.1 Project contextualization and motivation

The use of hydrogen as an energy source has been one of the most talked about subjects in the last few years as it is one of the possible energy source alternative to fossil fuels.

Although hydrogen use as a fuel source has its advantages, such as the reduction of pollutant emissions which inherently helps the environment, it is still viewed in the eyes of the public as a dangerous and unsafe fuel vector.

In order to study and implement a process that can charge hydrogen storage tanks that can be used in transport and mobility, this dissertation was presented by the research group led by professor Leonardo Ribeiro.

## 1.2 Objectives

The primary purpose of the current work is to develop and dimension a hydrogen storage system. It is intended to determine which materials are most suited for use in this application, as well as which components must be selected for the storage system to function as the research group intends. Due to the fact that each storage tank has its own unique characteristics, it was essential to determine the correct proportions for a quick, safe, and effective charging-up process of the tanks.

## 1.3 Methodology

The adopted methodology begins with the thick cylinder analysis, which was the favored method for calculating the internal and external diameters of hydrogen pipelines. These values were validated and filtered using the Tresca and Von Mises yield criteria of the selected material for the composition of the pipeline. The pressure loss was then calculated based on the length of the pipeline using the Darcy-Weisbach equations. Utilizing the same Darcy-Weisbach method, the local pressure loss in standard pipeline components such as valves and elbows was determined.

## 1.4 Structure of the dissertation

The present dissertation is divided into 6 groups. The first category includes the contextualization and introduction of the thesis's objectives. In the second group, a literature study is conducted about hydrogen, its usage as a fuel source, and various storage methods. In addition, a variety of materials that are compatible with hydrogen operations were investigated, as well as key components of hydrogen piping systems, such as compressors and valves. The third group gives the problem description and prior study conducted by the research group that presented the dissertation's theme. In the fourth section, the methodology and considerations used to find a solution to the issue are described. The findings discovered are presented in the fifth chapter. In the sixth and final group, some conclusions drawn from the acquired findings are presented.

# Chapter 2

# Literature review

## 2.1 Hydrogen

Hydrogen is the element represented by the letter $H$ in the periodic table. It is the lightest element as it is constituted by only one proton and one electron. Its molar mass is 1.00794 ua [1]. At the normal pressure and temperature conditions (NPT conditions), hydrogen is found in gas form ($H_2$), which is colorless, odorless, and non-toxic.

Since this is the most common element in the universe, and it has one of the biggest specific energies, it has become a source of a lot of discussion for the production and storage of energy. Due to the use of fossil fuels triggering a slew of major environmental issues and their eventual scarcity in the next decades, research into alternative energy sources other than fossil fuels has become critical. The research on renewable energy sources such as the sun, wind, and tides, among others, has been very significant for eco-friendly overall energy production.

Hydrogen has some properties that make the gas very suitable for energy production and storage. The amount of energy per kilogram of hydrogen, otherwise known as gravimetric energy density (GED), is very high [2], making the gas a good energy storage candidate. However, its density is very low. These features highlight some of the benefits and drawbacks of using hydrogen as a fuel [2].

Various companies have invested in projects including hydrogen as its main form of energy production and storage: such as the Hyundai Nexo and the Toyota Mirai, both vehicles have been mass-produced and sold to the public. These, among others, are some of the examples of how hydrogen can be a reliable energy source or energy storage method.

## 2.2 Hydrogen Storage

Hydrogen can be stored as a gas, a liquid, or even absorbed in a metal. There are various obstacles when it comes to hydrogen storage since the volumetric energy density (VED) is very low in comparison to most fuels, as it can be seen in Figure 2.1. Either there needs to be a reservoir with a lot of volume or high pressure to store hydrogen which brings a lot of efficiency problems since

there is energy spent in achieving those high pressures and, for certain applications, there are no storage tanks with high volumes. The next section explains some hydrogen storage methods as well as it describes some of their advantages and disadvantages.

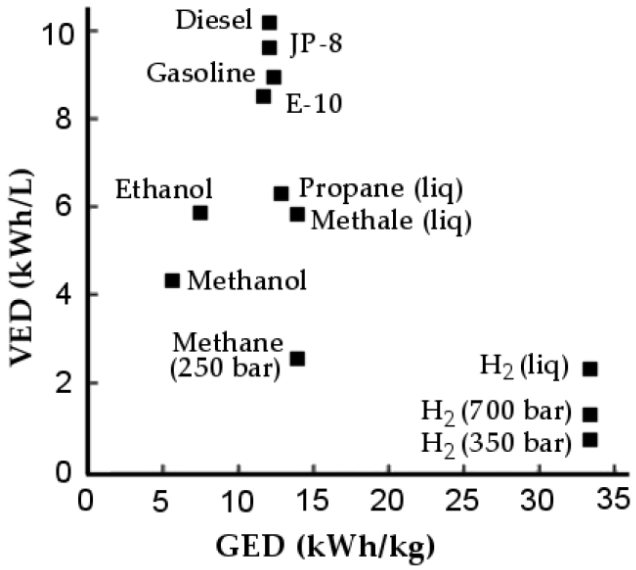



Figure 2.1: Comparison between the GED and VED for compressed hydrogen gas, cryogenic hydrogen, and other fuels [3].

### 2.2.1 Compressed gas storage

This is the most common method to store hydrogen as it is one of the easiest and simplest ways to do so. This process has its advantages as well as its disadvantages when it comes to safety, ease of use, and accessibility.

As previously stated, it is a simple method, as the pressurized cylinders are filled with the gas until the pressure inside reaches 200 to 300 bar (sometimes it can reach up to 700 bar). The deposits can be emptied, and refilled countless times (long lifespan) and the hydrogen stored in the containers does not need to be pure, no extra energy needs to be spent in purification.

However, hydrogen is a very highly flammable and volatile gas (certain mixtures between hydrogen and atmospheric air can result in detonation) and when hydrogen burns the flame is invisible. Nevertheless, its high buoyancy, low density, and its high molecular velocity make it so that the hydrogen disperses vertically in a short period of time, so when there are accidents or leaks, it is easier to predict and control the reaction.

One of the main problems of compressed hydrogen gas storage is its high leakage which is 3.3 times bigger than the air. The ease of loss of gas can lead to security and safety problems. The materials chosen for the pressurized materials need to seal all the fuel at high pressures inside without leaks.

Furthermore, the possibility of diffusion of the atomic hydrogen into the material of the internal walls of the reservoir or piping system should be avoided. The reaction that occurs between some carbonaceous metals, such as steel, with hydrogen cause the generation of $CH_4$ bubbles which can cause in small voids that can lead to cracks or fissures in the steel. This phenomenon is called hydrogen embrittlement and it is well known and studied. To combat this problem, some chromium rich steels have been found to be resistant to this corrosion effect [4].

So, to summarize:

- Pros:
  - Simple and reliable storage method, pressurized tubes have a long lifespan.
  - High specific energy (GED, high amount of energy per kg of hydrogen).
  - Hydrogen does not need to be pure.
  - High buoyancy and molecular velocity make hydrogen disperse in a short period of time.
  - Low density makes it so that the hydrogen gas scatters upwards.
- Cons:
  - Highly volatile and flammable gas that reacts easily with air.
  - Low energetic density (VED, due to the low density of hydrogen, there is needed high pressures or big volumes).
  - Invisible flame
  - Hydrogen can be lost very easily due to its high permeability
  - Hydrogen embrittlement

### 2.2.2 Cryogenic liquid storage

The storage of hydrogen in its liquid form is useful when the amount of hydrogen that needs to be stored is very large, since the liquid hydrogen (most commonly known as LH2) is stored at only 3 to 5 times the atmospheric pressure. The main disadvantage of this storage technique is that it requires a temperature of around 22K (-251°C) for hydrogen to be liquid. To sustain such a temperature, a significant amount of energy must be expended, significantly decreasing the process energetic efficiency. The energy losses can be up to 45%.

Despite the density of LH2 being higher than the gaseous hydrogen (which increases its VED and helps with storage), the evaporation that naturally occurs depending on the heating loads that hit the cryogenic hydrogen, makes it so there are small fuel losses.

When it comes to safety precautions and regulations, liquid hydrogen has its advantages and disadvantages. As it is a cryogenic liquid, it cannot be in contact with the human skin (it can cause frostbite) and other serious injuries. All the cables and components that are in direct contact with the liquid hydrogen need to be carefully insulated to prevent fuel losses due to evaporation. Also,

further insulation is needed to prevent the surrounding air to condensate and to eventually contact liquid hydrogen, which can lead to an explosive mixture. However, in case of leaks or accidents the liquid will stay in place and slowly escape the reservoir that it is inside [4].

So, to review

- Pros:
  - Better density than compressed hydrogen, allows for more storage in the same area.
  - Method most used for storage of high amounts of fuel.
  - In case of failure or accident the liquid hydrogen will stay in place and slowly evaporate.
- Cons:
  - Must be stored at 22K, which involves energy losses.
  - If there is a high heating load on the containers (especially if they are not well insulated) there is fuel loss due to evaporation.
  - High amount of insulation needs to be done in order to protect human skin from the cryogenic liquid.

### 2.2.3 Reverse metal hydride storage

This is an alternative method to store hydrogen. Certain metals and alloys (M) can mix with hydrogen forming a metal hydride. To obtain this hydride, a generic reaction equation 2.1 can be represented.

$$M + H_2 \leftrightarrow MH_2 \tag{2.1}$$

From the left to the right, this reaction is exothermic, which means that when the hydride is forming it releases some energy in form of heat. The pressure at which the hydrogen is stored is relatively low, around 2 bar. When hydrogen needs to be extracted from the hydride the opposite reaction needs to happen, heat is provided to the hydride lowering the pressure and releasing the stored hydrogen.

This method has certain advantages that make it very optimal for hydrogen storage such as its safety: hydrogen is stored at relatively low pressures so there are no rapid discharges; its lifespan is also one of its main advantages: usually there can be done multiple hundreds of charging and discharging cycles.

However, some disadvantages arise when utilizing this storage method. Hydrogen needs to have a high level of purity in order to not inflict damage to the system; the time to charge and discharge are very long, one hour for 5 kg of $H_2$; when there's charging and discharging certain temperature conditions need to be met (for charging there is needed low temperatures, since the reaction is exothermic, and for discharging there needs to be high temperatures since the reaction is endothermic) [4].

So, to recap:

- Pros:
  - Very safe, hydrogen stored at low pressures. There are no rapid discharges
  - Storage method with a very high lifespan.
  - Self-regulating storage method, for discharge there is needed high temperatures so when there are failures the hydrogen does not escape the hydride.
- Cons:
  - $H_2$ needs to have a high level of purity.
  - Charging and discharging times are very long.
  - For charging there is needed low temperatures to maintain the pressure stable. For discharging there needs to exist high temperatures because of the endothermic reaction.

### 2.2.4 Other methods

There are other methods to store hydrogen that vary from chemical processes to carbon nanofibers. These methods are still under research to be perfected. As it is not the main intent of this thesis to discuss such methods they will not be explained. Note that these methods are still very recent or haven't been made efficient enough to be considered reliable energy storage techniques.

## 2.3 Spheres storage method

The main inconvenience of compressed gas hydrogen storage is the safety concern regarding the use of high pressure. As a way to avoid the usage of this type of method, the research group has proposed the storage of high-pressure hydrogen inside small spheres inside a low-pressure container, as it can be seen in Figure 2.2.

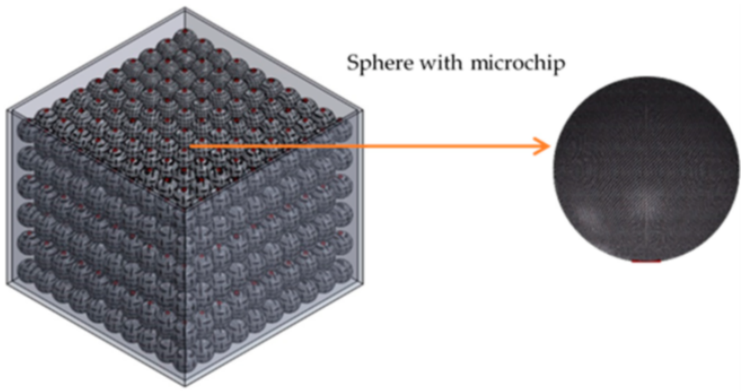



Figure 2.2: Proposed storage system [5].

The spheres are constituted by two layers, one outer structural layer and one inside liner, and a silicone microchip that regulates the entrance and exit of hydrogen[6; 7].

It was investigated the usage of several materials in the various layers of the macrospheres[8]. Carbon fiber epoxy was chosen as the best material for the exterior layer, ensuring that the spheres can withstand the tremendous pressure of the hydrogen within. And the optimum material for the interior layer, aluminum, prevents considerable hydrogen loss by permeation [8].

The proposed method of storage is suited for use of hydrogen as a fuel source. The storage tanks can be used in vehicles such as trucks and cars.

It was also compared the macrospheres storage technology to the storage methods utilized in the Toyota Mirai and the Hyundai Nexo [8]. The comparison was conducted by comparing the different GED, VED, weight, and mass of hydrogen contained in the system. Figures 2.3 and 2.4 depict the various results of this comparison, which demonstrate that the use of the macro-spheres storage technique is favorable in certain aspects while also depicting some of its limitations [8].

As shown in Figure 2.3, the GED on the macro-spheres method is substantially higher (151%-278%), which is due to the system's smaller mass (77%-87%). The outer storage tank is only designed to sustain roughly 5 bar of pressure, whereas the tanks in the Hyundai Nexo and Toyota Mirai are designed to endure pressures of up to 700 bar, implying heavier and more sophisticated materials [8].

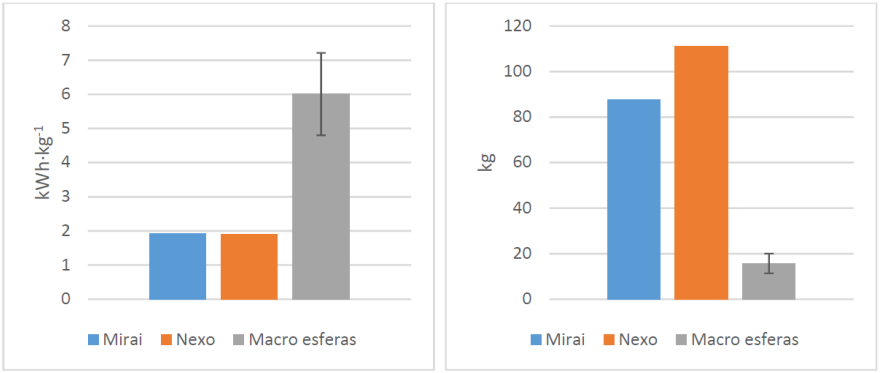



Figure 2.3: On the left, GED and, on the right, weight comparisons [8].

However, as compared to the state of the art, not all characteristics of this storage method are improvements. The VED and the mass of hydrogen stored are compared in Figure 2.4, and the core issue with hydrogen usage for fuel purposes remains unresolved, which is the VED value. The VED in the macro-spheres approach is lower (36%-56%) because the volume contained in the spheres is less than in the other storage techniques. Because there is less hydrogen available for consumption, the vehicle's autonomy decreases. One method to avoid this is to improve the packing of the spheres inside the tank. Studies in this area of expertise should be conducted in order to better allocate more hydrogen inside the tank.

It was also investigated the prices of different storage techniques and concluded that the Toyota Mirai, for smaller distribution series, would cost roughly 28 €/kWh [8]. Taking into consideration

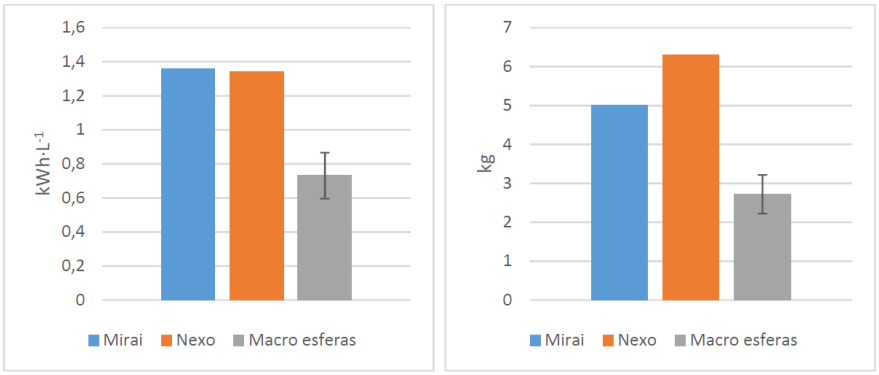



Figure 2.4: On the left, VED and, on the right, Stored Hydrogen Mass [8].

the cost of the various components and materials, the expenses for the macro-spheres storage technique would be between 11.69 and 14.77 €/kWh, a reduction of 47% to 58% compared to the state of the art [8]. When it comes to autonomy the spheres method offers only about 292 to 422 km. The Toyota Mirai has an autonomy of about 550 km. The loss in autonomy is about 23% to 47% [8].

### 2.3.1 Components

All the components in a hydrogen charging system must adhere to particular specifications due to the gas's characteristics, which have previously been stated above, such as molecular permeability, and application requirements, such as operating pressure and temperature. All materials and component types must be chosen in accordance with these standards.

#### 2.3.1.1 Material Selection for the piping system

The piping system allows hydrogen to be charged into the storage tank. It must be able to endure the high pressures and corrosion caused by the gas. In terms of materials, the piping system may be made of both metallic and non-metallic materials. Metallic materials are better suitable for major structural parts, whilst non-metallic materials are better suited for small and functional components.

- Metallic Materials:

  The permeation of hydrogen is one of the biggest reasons why the metallic materials are used in the piping systems' main pipelines since these materials have a negligible loss of hydrogen through permeation. The fundamental issue with these materials is their resistance to corrosion, specifically their resistance to hydrogen embrittlement. This phenomenon is heightened when the working pressures are bigger.

  The preferred maximum hardness of these materials should be 22 HRC or 250 HB. Materials that have a very high hardness level should be avoided since they are more susceptible to corrosion and are harder to machinate which decreases their usability. Components that are

made of alloys with a fine grain and that don't contain internal or superficial defects should be selected [9].

- Carbon Steels

  Known to be the most used type of steel, carbon steels are good for applications that do not operate with high pressures. Since this type of steel doesn't have high strength values corrosion resistance is good, which means that hydrogen embrittlement does not happen as frequently. For these types of steel, the maximum tensile strength value should be 800 MPa. The selection of these types of materials should have the lowest value of tensile strength in mind to obtain the best resistance to hydrogen embrittlement [9].

- Low-Alloy Carbon Steels

  These steels are used in applications involving high temperatures and corrosive environments. Their welding process is very difficult. The weld is usually very hard and brittle, and very susceptible to hydrogen embrittlement. The alloys employed in these steels, such as manganese, sulfur, phosphorus, and chromium, are often associated with a higher susceptibility to hydrogen embrittlement [9].

- Austenitic Stainless Steels

  This is the category of steels that is most resistant to hydrogen embrittlement, which, along with their superior mechanical qualities, makes them the best suited for high-pressure applications, since they provide the best performance among metallic materials.

  These steels are only vulnerable to hydrogen embrittlement when their composition undergoes phase transition. The hydrogen embrittlement phenomena can occur during the production of ferrite or martensite. However, these phases only develop when the steel is subjected to extremely hard conditions, such as extremely high strain values.

  The percentage of alloys in these steels is critical since their resistance to hydrogen embrittlement is highly reliant on their presence. For example, the larger the quantity of nickel in the steel is usually correlated with stronger resistance to hydrogen embrittlement [9].

- Aluminium Alloys

  Because the hydrogen gas must be exceedingly pure to avoid hydrogen embrittlement, the applications for these alloys are relatively limited. The hydrogen embrittlement phenomenon occurs when hydrogen gas contains water vapor, which raises the hydrogen's solubility in the aluminum. Because of this issue, the purity of the gas must be strictly controlled so that no fissures occur in the material [9].

- Copper Alloys

  It is not a widely utilized material in hydrogen transportation, yet it possesses one of the highest hydrogen permeability values. Because of this feature, cooper alloys are

highly reliable for insulating applications or components. One of the primary issues with copper-based hydrogen transportation is the presence of oxygen in the hydrogen flow, which can induce the formation of oxides that degrade the mechanical qualities of the copper, resulting in fissures [9].

- Non-Metallic Materials

  Non-metallic materials are not used for hydrogen transportation or storage. These materials present very high values of hydrogen permeation, making them good fits for membranes, for example. However, in hydrogen pipelines they can be used for external components, i.e., components which are not in contact with the hydrogen gas.

  Some of these materials have a very low working temperature limit, such as some resins and plastics, making them unable to be used in these situations. Some examples of these materials are shown below on Table 2.1 [9].

Table 2.1: Working Temperature Limit of some common plastics [9].

| Plastic | Temperature Limit [ºC] |
|---|---|
| Plasticized cellulose | 20 |
| Cellulose diacetate | 20 |
| Formo-aniline | 20 |
| Formo-urea | 20 |
| Phenol-formaldehyde | 20 |
| Furaphenol | 20 |
| Polyamides | 20 |
| Polyfuran | 110 |
| Polychloroprene | 100 |
| Polyepoxydiphenylopropane | 90 |
| Polyethylene glycol terephtalate | 20 |
| Polyurethane | 20 |
| Polyurethylmethacrylate | 20 |
| Polyvinyl acetate | 20 |
| Polyvinyl chloride | 60 |
| Polytrifluorochlorethylene | 180 |
| Polytetrafluoroethylene | 250 |
| Polyethylene | 60 |
| Polyisobutylene | 100 |
| Polystyrene | 20 |
| Polyacrylonitrile | 20 |
| Polyvinyl-vinylidene chloride (20-80%) | 60 |

These materials are not used in structural applications due to their low strength and stress resistance. They would not be able to withstand the immense pressures.

Some elastomers are compatible with hydrogen gas, however they present high values of permeation, as it can be seen in Table 2.2 [9].

Table 2.2: Permeation Values of some Elastomers [9].

| Elastomer | Permeation Value x $10^{-9} cm^3_{STP}.cm.s^{-1}.cm^{-2}.(cmHg)^{-1}$ |
|---|---|
| Natural rubber | 492 |
| Butyl rubber | 74 |
| Buna S ® | 399 |
| Perbunan ® G | 158 |
| Neoprene ® G | 133 |
| Hycar or 15 ® | 74 |
| Polybutadiene | 424 |
| Polymethylpentadiene | 428 |
| Perbunan 18 ® | 251 |
| Isoprene-methacryl-nitrile copolymer | 138 |
| Hycar or 25 ® | 118 |
| Polydimethylbutadiene | 172 |
| Vulcoprene A ® | 64 |
| Isoprene-acrylonitrile copolymer | 74 |
| Thiokol S | 16 |

#### 2.3.1.2 Compressors

The compression process is required to obtain the necessary pressures in the storage tank. This is accomplished by using a compressor to increase the input pressure of the hydrogen gas to the appropriate output/storage pressure. There are two types of compressors; mechanical and non-mechanical compressors.

- Mechanical Compressors

  They are the most widely used compressors due to their ease of use, technological maturity, ease of maintenance, and overall low cost. Their principle is based on the reduction of a closed volume, increasing gas pressure, and ensuring no leaks.

  These compressors are used in a wide variety of operating pressures, ranging from a few bar to hundreds of bar. A different type of compressor should be used depending on the desired pressure. The diaphragm and piston compressors are the types of compressors that should be utilized for high-pressure delivery applications, as shown in Figure 2.5.

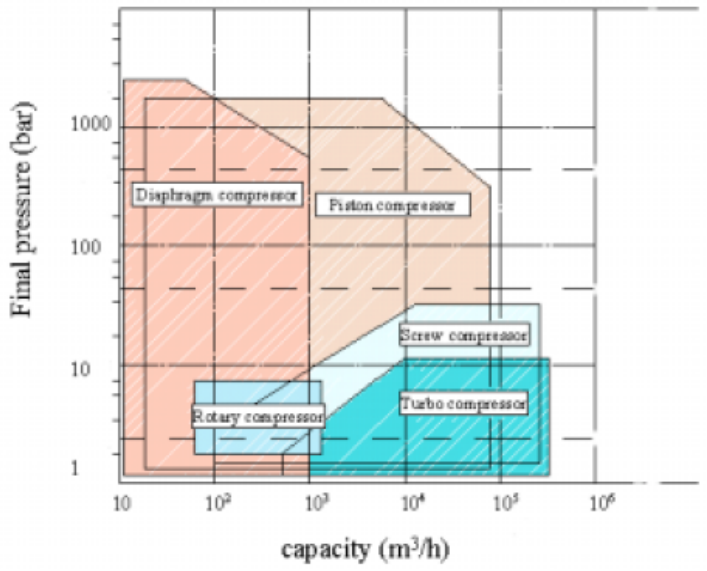



Figure 2.5: Discharge pressure vs Compressor's capacity [10].

– Reciprocating Piston Hydrogen Compressors

The construction of the piston compressors is shown in Figure 2.6. The piston has a cyclical movement imposed by the crank and the connecting rod which are moved by a motor, and compresses the gas that is inside the cylinder. When the pressure of the hydrogen reaches a threshold value, the exit valve is forced open by the gas and the piston is moved down, restarting the cycle again [10].

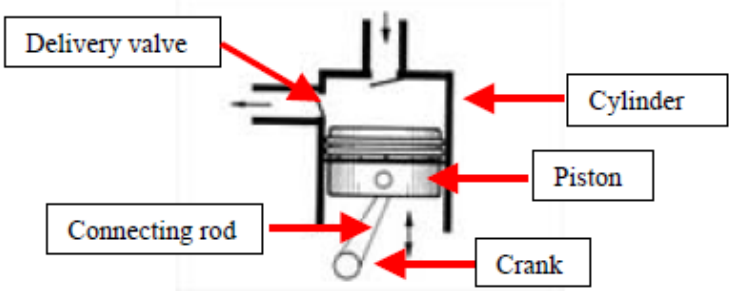



Figure 2.6: Schematic of a single-acting reciprocating piston hydrogen compressor [10].

These compressors often have compression ratios of 4:1 or 3:1, which is more than adequate for light applications. However, multistaged compression is required for high pressure needs. It has previously been demonstrated that multi-stage compression is more efficient than single-stage compression for these sorts of procedures [10].

Because of the nature of this compression process, the materials suffer a lot of wear and tear due to friction induced by the constant motion. Frequent lubrication and maintenance are essential to overcome this issue. The compressor's lifespan is directly correlated with the type of lubrication that is done. When there's a frequent lubrication

done some compressors can reach up to 3 years of use. However, when there is no lubrication done, the compressor's lifespan is reduced to only 6 months [10].

The materials employed in these compressors must be able to withstand both the pressures generated and the embrittlement phenomena induced by the hydrogen gas, as detailed in the preceding sections. Because they are resistant to these difficulties, stainless steels and alloy steels rich in chromium and molybdenum are suggested metals for the design of these compressors, as opposed to carbon steels, which gain fractures that generate ruptures that lead to possible leaks [10].

– Diaphragm Compressors

These compressors work on the following principle: as illustrated in Figure 2.7, the hydrogen gas is compressed by the oscillating movement of a sandwich-type metallic membrane within a double concave encasing. The membrane moves due to the cyclical movement of a piston, which elevates the pressure of a hydraulic fluid on one of the membrane's sides. The hydrogen gas, on the other side, is compressed due to the volume change, and when the gas pressure reaches a certain value, the exit valve opens, allowing the compressed hydrogen to escape. After the hydrogen exits the compartment, the piston reverses its motion, allowing decompressed hydrogen to enter the compartment and continue the cycle [10].

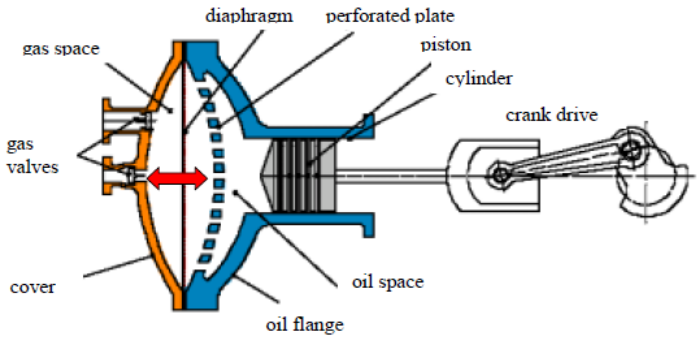



Figure 2.7: Schematic of a diaphragm compressor [10].

The leakage value of the compressors is substantially lower as compared to piston compressors since the metallic membrane is sealed between the two casings. Because the hydrogen gas does not come into touch with the hydraulic fluid, assuming the compressor's membrane does not tear, the purity levels of the gas remain unchanged [10].

These compressors have compression ratios ranging from 15:1 to 20:1, although their flow rate is only approximately 200 $m3/h$. The number of compression stages required to attain a specific pressure for high pressure hydrogen supply is reduced [10].

#### 2.3.1.3 Valves

In order to materialize the charging system, valves need to be chosen accordingly to the specifications imposed not only by the hydrogen gas but also the working pressures that are present in this application.

Valves for this type of hydrogen service need to be made of a material that can withstand both the immense loads caused by the pressures inside the pipelines and the hydrogen embrittlement phenomenon. As it was explained before, 316L stainless steel would be a good candidate since it can provide good mechanical properties and good resistance to the corrosion by the hydrogen. Many hydrogen valve manufacturers use this steel as the main component of their valves, such as High Pressure Equipment®, a specialized company in hydrogen pipeline accessories such as fittings, valves and pressure vessels [11].

Valves can be categorized by their function and constructive type. The valves explored in this dissertation will be the Non-Return and Flow-Control valves since they are the types of valves that are needed.

Non-return valves are used to prevent backflow of the working fluid. These valves are used to safeguard equipment and mechanisms from potential reverse flows. When reverse flow develops, bearings and gears will be the primary components harmed. And due to the inability of some equipment to work in reverse, such as some compression machines, reverse flow in may create catastrophic machine malfunctions.

These valves, such as swing disc valves (Figure 2.8), piston valves (Figure 2.9), ball and diaphragm valves, are designed to function according to the equilibrium between the fluid-dynamic forces and the weight of the seal or seat utilized in the valve.

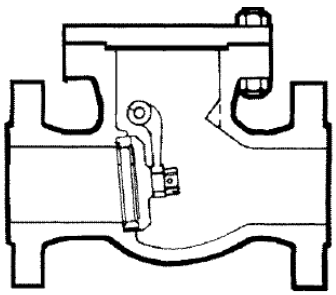


Figure 2.8: Typical one-piece body cast swing disc non-return valve [12].

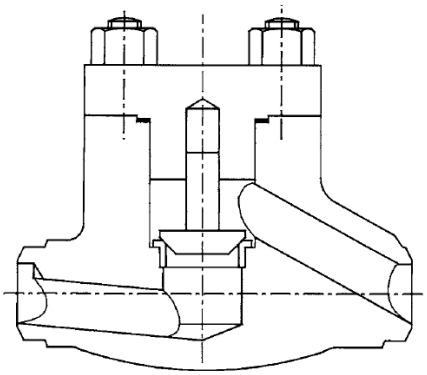


Figure 2.9: Typical closed piston non-return valve [12].

Controlling fluids in pipe systems requires the use of control valves, which are activated by actuators that are directed by a controller that defines the desired fluid conditions. These commands are often the result of a comparison between the fluid's real-time conditions as measured by a sensor and the conditions that are expected to be satisfied [12].

Control valves control fluid flow, which affects the pressure and flow rate of the fluid after the valve. Various construction styles of these valves allow them to be employed in various circumstances; thus, their functioning criteria should be already stated, such as, operational function, the fluid to be regulated, the input pressure, pressure drop, flow, maximum noise level, leakage, and size [12].

These valves can be divided into two different groups, depending on their actuator motion: rotary or linear. The actuators for these valves can use compressed air, electricity or hydraulic fluid as means of action. Rotary motion actuators are employed in rotary plug valves, ball valves and butterfly valves (Figure 2.10). While linear motion actuators are employed in globe (Figure 2.11), gate, and cage valves [12].

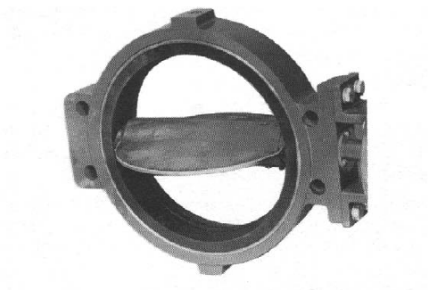


Figure 2.10: Butterfly valve [12].

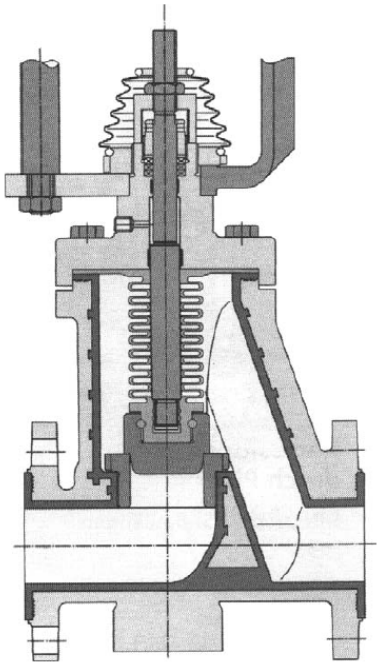


Figure 2.11: Lined single-seat globe valve [12].

fort the rotary motion actuating valves it was studied that: the plug valve is a plug-shaped disc with a horizontal passageway bored through it. It is not suitable for throttling duties, thus it is only utilized for on and off states; the ball valve is a quarter-turn rotary motion valve. It is a ball-shaped device used to initiate and halt flow. It is a quick-acting kind that is more compact and tighter than the gate valve (provides better shut off); the butterfly valve is a rotational motion quarter-turn valve. It consists of a disc-shaped component supported by a rod, and it controls, regulates, and stops the flow. It is very lightweight, simple to install, and capable of withstanding high pressures. It is used primarily for large-diameter pipelines where gate valves are inconvenient [12].

For the linear actuating valves is was discovered that: the globe valve are used to manage the flow rate of a certain pipe system by stopping or regulating the flow. Due to the structure of these valves, leak tightness is one of its primary characteristics; the gate valve is the most prevalent sort of valve and is used in all services and applications. As they operate in an on/off way, they give effective shut-off [12].

# Chapter 3

# Problem Description

## 3.1 Tank Dimensions

These tanks will be utilized as fuel tanks for hydrogen powered storage trucks. Two types of these tanks were idealized based on the typical sizes of these machines' fuel tanks.

- Type 1 tanks

  These tanks are mounted on the truck's chassis, just like the standard varieties of diesel tanks.

  These tanks are replaced at the swap station with others that are already fully charged, using two robotic elevators (one on each side) that elevate from below the ground. This process is depicted in Figure 3.1.



Figure 3.1: Tank 1 swap procedure

- Type 2 tanks

  They are a new style of tank designed to be placed behind the truck's cab. The operation begins when a robotic arm rises from the truck's side, extracting empty tanks and replacing them with previously charged ones. Figure 3.2 illustrates this procedure.

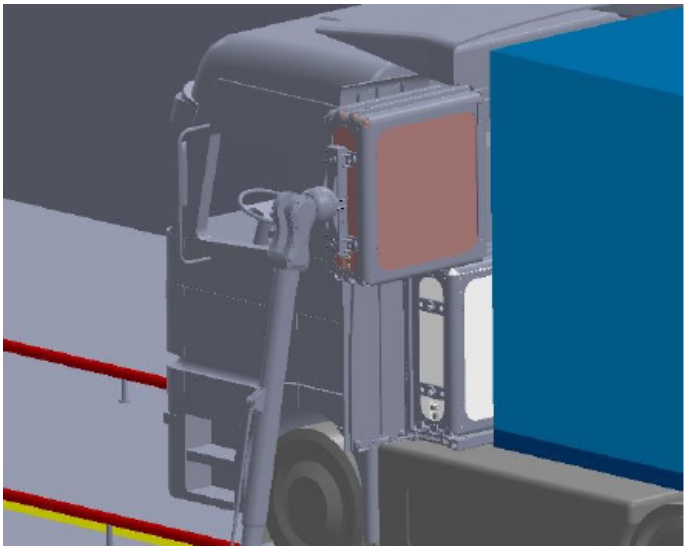


Figure 3.2: Tank 2 swap procedure

In Table 3.1, a comparison is made between the two types of tanks regarding dimensions, volume, number of macro spheres per tank, mass of hydrogen that can be present in the tanks of the truck.

Table 3.1: Dimensions, Number of spheres, Mass of hydrogen of each type of tank

| | Internal dimensions | | | Volume (l) | Macro-spheres/tank | Mass H2/tank (kg) | Tanks/Truck | Mass H2/truck (kg) |
|---|---|---|---|---|---|---|---|---|
| | L | H | W | | | | | |
| Tank type 1 | 1536 | 675 | 675 | 699.84 | 4889 | 21.55 | 2 | 43.10 |
| Tank type 2 | 1085 | 386 | 1127 | 472.00 | 3137 | 13.83 | 4 | 55.32 |
| | | | | Total Truck: | 22326 | | | 98.42 |

This table indicates that two tanks from the type 1 version would be put in the truck's chassis and four tanks from the type 2 variant would be mounted on the rear of the cab. When completely charged, these tanks would amount to around 22326 spheres per truck, equaling 98.42 $kg$ of hydrogen gas.

## 3.2 Charging/discharging methods

There are two ways that can be used for the charging and discharging of the storage tank proposed by the research group: using water and using air. The vehicle goes to the charging station, leaving its empty tank behind, and taking away a full one. The charging procedure is carried out below ground in order for the charging chamber to withstand the pressures within it.

- Water A1: Water is used to achieve pressure equilibrium since pressures close to 1000 bar will be generated inside the storage tank and the charging chamber, as it is demonstrated in Figure 3.3. The storage tank has one hose that will direct the hydrogen inside. Firstly, the tank arrives at the charging station and all the air inside it needs to be removed. Water is then pumped inside the charging chamber, and after all the air is outside of the charging chamber the air exit valve is closed.

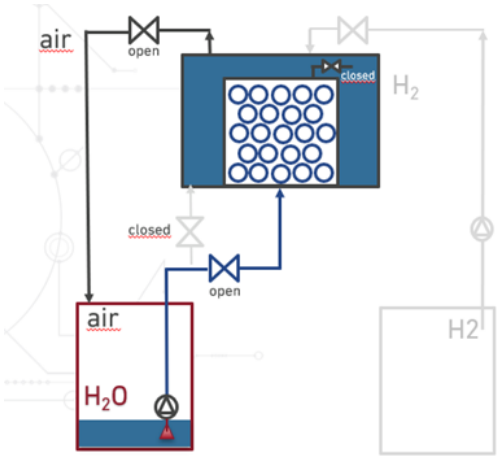



Figure 3.3: Water A1 solution - first step

After that, all the water is then returned to the source tank pushed by the hydrogen that has commenced to enter the charging. The gas is then pumped inside the charging chamber, Figure 3.4, and the hydrogen trap prevents the gas from going inside the water source tank. For the hydrogen to get inside the storage tank the valve on the hose that is connected to the tank is open.

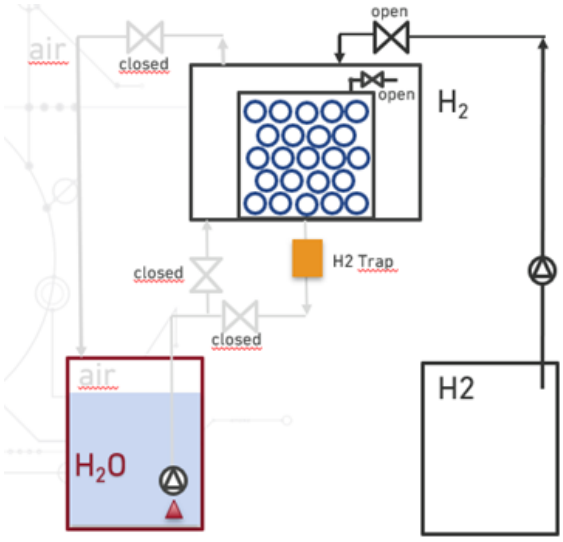



Figure 3.4: Water A1 solution - second step

The charging chamber and the storage tank are then supercharged meaning that the pressure inside those elements will reach the desired 1000 bar. In this step, the spheres open their silicon microchip, and the storage tank charging process begins. After the charging process ends, the hose valve is closed, Figure 3.5, and then water is pumped inside the charging chamber expelling the remaining hydrogen to its source tank.

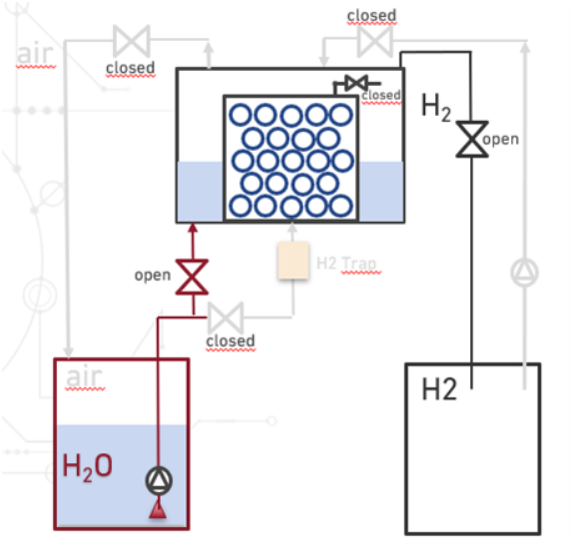



Figure 3.5: Water A1 solution - third step

After the hydrogen has been entirely discharged from the charging chamber, the water is pumped out, leaving the storage tank ready for removal from the charging station. The storage tank is now ready for usage, as it can be seen in Figure 3.6.

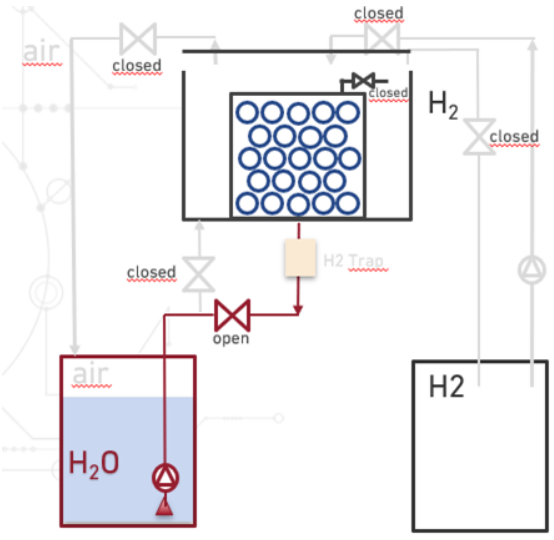



Figure 3.6: Water A1 solution - fourth step

- Water A2: This second charging technique is safer since the hydrogen and air never share

the same reservoir, making the procedure significantly better and preventing dangerous interactions between residual air and hydrogen, which can be very harmful to the system.

When the storage tank is mounted within the charging chamber, a hose connects the storage tank to the outside hydrogen transportation pipe. The hydrogen never fills up the charging chamber in this process.

The air inside the charging chamber is removed in the same way that it was removed in the previous procedure, namely by pumping water inside and expelling all of the air.

It should be noted that pressure switches are utilized in the solution to activate when the necessary pressure is reached. One switch is for water, while the other is for hydrogen, as it can be seen in Figure 3.7.

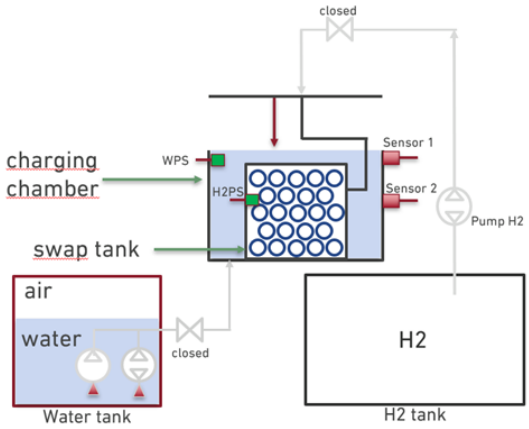



Figure 3.7: Water A2 solution - first step

After all the hydrogen has been evacuated from the charging chamber, the water must be pressured for the storage tank to handle the pressures created.

Then hydrogen begins to be inserted into the storage tank and the charging process begins, Figure 3.8.

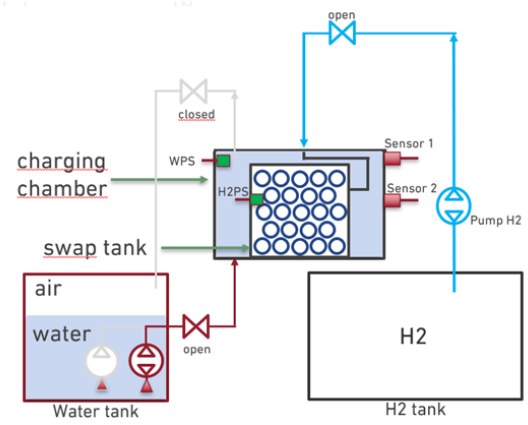



Figure 3.8: Water A2 solution - second step

The pressures inside the storage tank and charging chamber are controlled by the H2PS and WPS, respectively. After reaching the required pressures, the macrospheres seal their microchips, and the depressurization of both tanks begins, Figure 3.9.

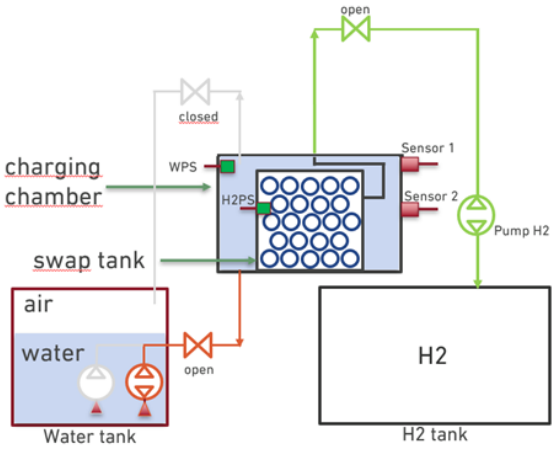



Figure 3.9: Water A2 solution - third step

The storage tank is ready for use once the hydrogen has been discharged and the water has been removed from the charging chamber.

- Compressed air:

  This charging method is very similar to the previous solution. In this case, since there is only air and hydrogen involved, the possibility of failure due to hydrogen and air reaction is augmented. However, this technique doesn't allow the hydrogen and the air to mix if the system works properly. Firstly, the storage tank arrives at the charging station and a hose connects it to the hydrogen outside source. The charging chamber will only hold air during the charging process, Figure 3.10.

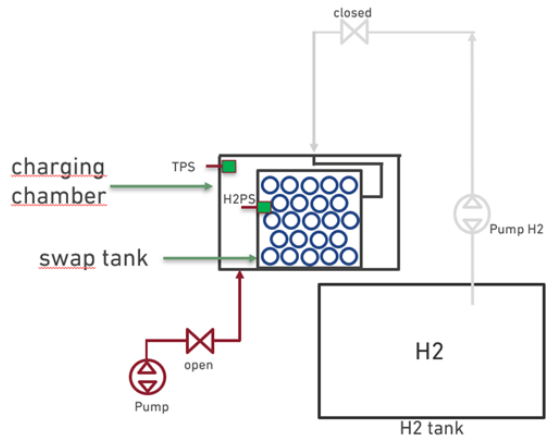



Figure 3.10: Compressed air solution - first step

The charging chamber and the storage tank are then pressurized until 1000 bar and the charging process begins with the macro spheres opening their silicone microchips. Figure 3.11. The pressure control is made with pressure switches (one for hydrogen, and another for air).

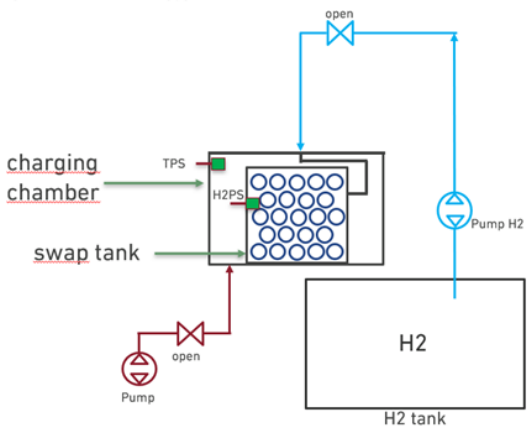



Figure 3.11: Compressed air solution - second step

Following the completion of the charging procedure, the charging chamber and storage tank are discharged, and the storage tank is ready to be withdrawn from the charging chamber and used, Figure 3.12.

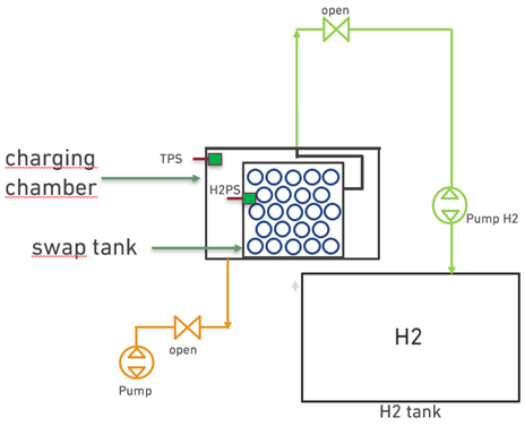



Figure 3.12: Compressed air solution - third step

All these charging methods are conceptual models, and many components, including pumps, piping systems, hoses, valves, and sensors, remain to be defined. Throughout this thesis, these aspects will be dimensioned.

## 3.3 Adopted spheres charging method

Due to the enormous pressures in the tanks and pressure system, charging the spheres in one step would be impossible. The stresses created would damage the spheres' more fragile and non-structural elements, such as the silicon chip and the inside walls.

The selected charging procedure begins with the establishment of one pressure differential, say 30 KPa, and proceeds in small steps. These steps are categorized by discharges of pressurized hydrogen inside the tank that goes into the spheres after. A flow control valve regulates this process. The non-pressurized spheres are first filled by opening the silicon chips, and when the pressure inside them rises by 30 KPa, the charging process is terminated by shutting the silicon chips. During the pause, the pressure inside the spheres of hydrogen stabilizes. The pressure outside the spheres is then increased, and the silicon chips reopen, enabling gas to enter the spheres and initiating the next step of the charging process. These operations are continued until the necessary final pressure of 1000 bar is achieved inside the spheres. The tank is depressurized at the completion of the procedure once the spheres have closed. Figure 3.13 illustrates three cycles of this process, note that this graph is purely didactic as its goal is to help understand the charging process.

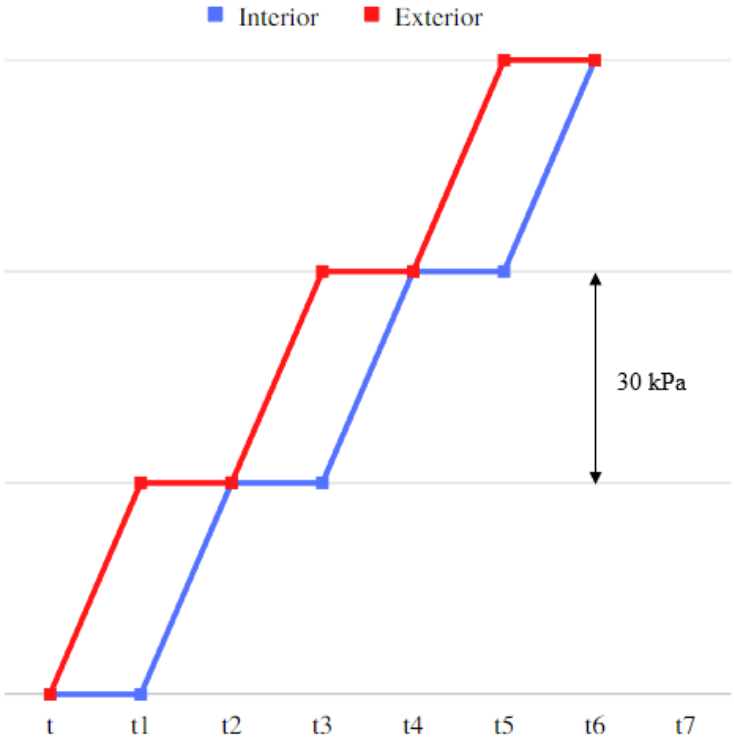



Figure 3.13: Pressure comparison between the interior and exterior of the spheres

There are no unexpectedly large stresses or strains in the materials of the spheres when this charging method is used. The hydrogen inside the spheres is adequately compressed and stored, and the process of filling the tank and the spheres occurs at a low and approximately constant temperature.

# Chapter 4

# Methodology

## 4.1 Hydrogen piping design

For the design of the hydrogen pipe system and the pressure loss calculation, it was assumed that the 316L stainless steel profiles supplied by HONGTU® would be used for the piping system and all of its major pipelines. The consequent physical and mechanical properties of the steel that were used for calculations were provided by Ramada Aços®.

The mechanical properties of the stainless steel, as well as those of other characteristics of the selected steel, were used in the calculations described ahead. All required values are listed in Annex A.

### 4.1.1 Piping design

#### 4.1.1.1 Inner and Outer diameter calculation

First, for the computation of the inner and outer diameters, a thin cylinder analysis was performed to determine the appropriate range of values for the application under study. Due to the high pressures inside the tube (up to 1000 bar), thin cylinder analysis produced impractical or no solutions. Therefore, an analysis of thick cylinders was conducted, since thick cylinders can tolerate more pressure and load.

The study of thick cylinders was simplified due to the fact that the value of the internal pressure relative to the outside atmospheric pressure is very high. Assuming that the pipeline is above ground, the computation ignored the atmospheric pressure outside and only considered the 1000 bar pressure within.

Cylinders that have a thickness-to-interior-diameter ratio greater than 0.1 are considered thick cylinders . [13] This signifies that the thickness is comparable to the inner diameter of the cylinder. These cylinders can endure very high pressures.

This calculation was based on the hypothesis that the strain of the cylinder in the axial direction is independent of the radius of the cylinder, this means that the sections of the cylinder are kept plain after the loads are applied. And since the solicitation of the load is interior and/or exterior

the values of the stresses are independent of the angle of the study point in the cylinder, Figure 4.1 [13].

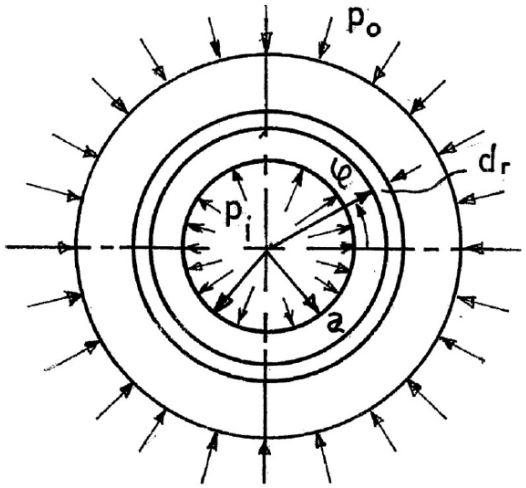



Figure 4.1: Thick cylinder, inner radius a and exterior radius b [13].

The axial stress, if it exists, is constant and independent of the radius, and is given by expression 4.1:

$$\sigma_l = \frac{p_i a^2}{b^2 - a^2} \tag{4.1}$$

Where $p_i$ is the internal pressure and $a$ and $b$ are the internal and external radius of the cylinder.

Considering both Figure 4.1 and the unit of length in the axial direction, there is:

$$2\sigma_t dr + 2\sigma_r r - 2(1\sigma_r + d\sigma_r)(r + dr) = 0 \tag{4.2}$$

Disregarding the second order terms of equation 4.2, there is:

$$\sigma_t - \sigma_r - r\frac{d\sigma_r}{dr} = 0 \tag{4.3}$$

Equation 4.3 relates $\sigma_t$ and $\sigma_r$, but to calculate their values, one must formulate an additional equation based on the assumption that longitudinal strain is constant. With the following Hook's law presented in equation 4.4:

$$\varepsilon_1 = \frac{1}{E}[\sigma_l - \upsilon(\sigma_r + \sigma_t)] \tag{4.4}$$

Where $\sigma_l$ is a constant, eventually null, $E$ is the Young modulus and $\upsilon$ Poisson's coeficient. Equation 4.5 can be written

$$\sigma_r + \sigma_t = 2C_1 \tag{4.5}$$

where $C_1$ is a constant, and from equation 4.3

$$r\frac{d\sigma_r}{dr} + 2\sigma_r = 2C_1 \tag{4.6}$$

Multiplying Equation 4.6 by $r$

$$r^2\frac{d\sigma_r}{dr} + 2r\sigma_r = 2rC_1 = \frac{d}{dr}(r^2\sigma_r) \tag{4.7}$$

Integrating Equation 4.7

$$r^2\sigma_r = r^2C_1 + C_2 \tag{4.8}$$

$$\sigma_r = C_1 + \frac{C_2}{r^2} \tag{4.9}$$

And from equation 4.5

$$\sigma_t = C_1 - \frac{C_2}{r^2} \tag{4.10}$$

Considering that the frontier conditions for $r = a$ $\sigma_r = -p_i$ and for $r = b$ both Equations 4.11 and 4.12 can be obtained:

$$C_1 = \frac{p_i a^2 - p_o b^2}{b^2 - a^2} \tag{4.11}$$

$$C_2 = \frac{a^2 b^2 (p_o - p_i)}{b^2 - a^2} \tag{4.12}$$

When there is no outside pressure the values of the circunferencial stress and radial stress are given by expressions 4.13 and 4.14, respectively:

$$\sigma_t = \frac{a^2 p_i}{b^2 - a^2}(1 + \frac{b^2}{r^2}) \tag{4.13}$$

$$\sigma_r = \frac{a^2 p_i}{b^2 - a^2}(1 - \frac{b^2}{r^2}) \tag{4.14}$$

In Figure 4.2 there can be seen the values of these stresses at the inside and outside of the cylinder as well as the stress distribution as a function of radius

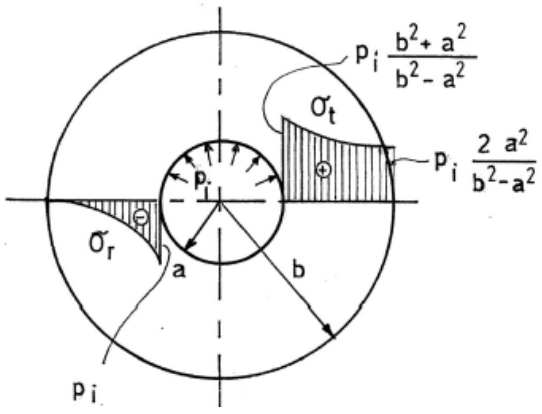



Figure 4.2: Stress distribution for a thick cylinder under internal pressure [13].

The maximum stresses occur in the interior wall of the cylinder, Euqations 4.15 and 4.16:

$$\sigma_t = p_i \frac{b^2 + a^2}{b^2 - a^2} \tag{4.15}$$

$$\sigma_r = -p_i \tag{4.16}$$

This previous calculation method and equations were based on the course notes by Paulo M.S.T. Castro [13]. Equivalent calculations can be found in other highly reputable books about the strength of materials such as the commonly known Féodossiev [14] and Timoshenko [15].

- Yield Criteria analysis

  Yield criteria are used in order to define the limit of elasticity under any combination of stresses. There are some different calculation methods that can be used, ones more restrictive than others, such as the Tresca method and the Von Mises method.

  Considering a thick cylinder only subject to internal pressure, and considering the last explanation on the distribution of the stresses, it can be concluded that internal wall of the cylinder will be the first part of the pipe to fail. Having the critical zone and its maximum stress values in mind the Tresca and Von Mises methods can be applied [16].

  The Tresca method implies that

  $$\sigma_1 - \sigma_3 = \sigma_e = \sigma_y \tag{4.17}$$

  In the particular case of the pipe only being subject to internal pressure $\sigma_1 = \sigma_{t_a} = p_i \frac{b^2+a^2}{b^a-a^2}$ and $\sigma_3 = -p_i$, so from Equation 4.17

  $$p_i \frac{b^2 + a^2}{b^2 - a^2} - (-p_i) = \sigma_y \tag{4.18}$$

  With this correlation, presented in Equation 4.18, arbitrating the outside and inside diameters of the thick cylinder it can be known if the pipe will withstand the internal pressure. $\sigma_y$ is a value characteristic of the material chosen for the pipe and $p_i$ is the internal pressure.

  On the other hand, the Von Mises method (Equation 4.19), also known as the maximum distortion energy method, and less restrictive than the Tresca method says that

  $$2\sigma_y^2 = (\sigma_t - \sigma_l)^2 + (\sigma_l - \sigma_r)^2 + (\sigma_t - \sigma_r)^2 \tag{4.19}$$

  Knowing the values of $\sigma_t = p_i \frac{b^2+a^2}{b^a-a^2}$, $\sigma_r = -p_i$ and $\sigma_l = \frac{p_i a^2}{b^2-a^2}$ the exterior and interior radius of the pipe and the equivalent stress of the material are the inputs of the equation.

### 4.1.2 Pressure loss

#### 4.1.2.1 Straight line pressure loss calculation

All the following calculation methods were studied and taken from the course notes by Carlos M.C.T. de Pinho [17].

The normal procedure for pressure loss calculation in the piping system is done with the use of the following Darcy-Weisbach equation (Equation 4.20), used for incompressible fluids:

$$\Delta p = f\frac{L}{D}\frac{V^2}{2}\rho \tag{4.20}$$

Where $\Delta p$ is the pressure loss, $L$ is the length of the pipeline, $D$ is the inner diameter of the pipeline, $V$ is the mean velocity of the fluid flow with $\rho$ density. $f$ is the dimensionless friction coefficient and it can be calculated using different methods depending on the characteristics of the material of the internal walls of the pipe and the nature of the fluid flow.

The energy equation for a steady incompressible flow is:

$$\frac{p_1}{\gamma} + \alpha_1\frac{V_1^2}{2g} + z_1 = \frac{p_2}{\gamma} + \alpha_2\frac{V_2^2}{2g} + z_2 + h_L \tag{4.21}$$

where $h_L$ is the head loss between sections (1) and (2), with the assumption that the pipeline is horizontal ($z_1 = z_2$) with constant diameter, which encompasses constant fluid average velocity, which can lead to:

$$h_{L,major} = f\frac{L}{D}\frac{V^2}{2g} \tag{4.22}$$

The difference between using equations 4.20 and 4.22 is that eq. 4.20 can only be used for horizontal pipes, while eq. 4.22 can be used for horizontal and slanted pipelines.

If the flow is laminar the $f$ coefficient is calculated using Equation 4.23:

$$f = \frac{64}{Re} \tag{4.23}$$

If the flow is turbulent and the fluid is being pumped through a pipe with smooth walls (low roughness) $f$ is given by Equation 4.24:

$$f = \frac{0.3164}{Re^{1/4}} \tag{4.24}$$

In the case fluid flow is turbulent and the internal walls have high roughness it is used the Colebrook formula (4.25) or the Moody diagram, Figure 4.3, (which represents graphically the Colebrook formula):

$$\frac{1}{\sqrt{f}} = -2.0\log\left(\frac{\frac{\varepsilon}{D}}{3.7} + \frac{2.51}{Re\sqrt{f}}\right) \tag{4.25}$$

Where $\frac{\varepsilon}{D}$ represents the relative roughness of the internal wall of the pipe, $Re$ is the Reynolds number and $f$ is the friction coefficient.

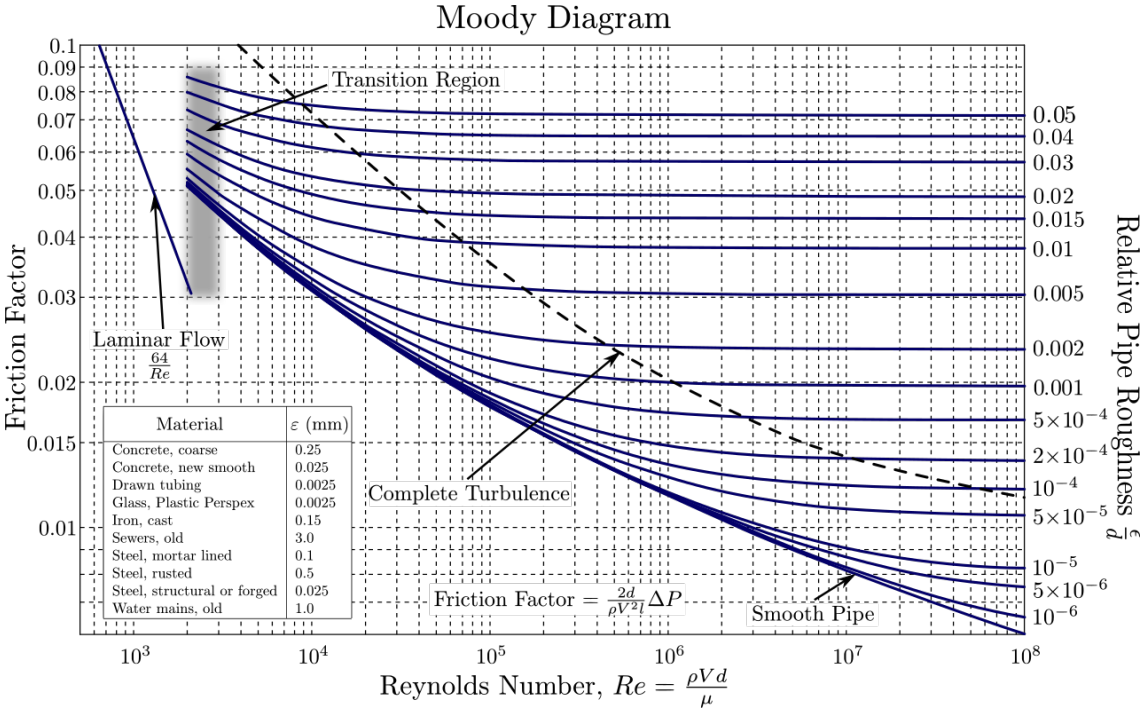



Figure 4.3: Moody Diagram [18].

The pressure loss calculation is made based on the principle that there are no turns, bifurcations, valves, or changes in interior diameter in the piping system. These phenomena have a large impact on pressure loss and should be accounted for.

#### 4.1.2.2 Local pressure loss calculation

All the following calculation methods were studied and taken from the course notes by Carlos M.C.T. de Pinho [17].

Equivalent lengths were determined for these components and the total $L$ of the pipeline is calculated according to Equation 4.26:

$$L_t = L_r + L_{eq} \tag{4.26}$$

Where $L_t$ is the total length, $L_r$ is the real length of the pipeline, and $L_{eq}$ is the sum of the equivalent lengths of the various situations that require them. There are various tables and formulas that provide the values of $L_{eq}$ of different valves, turns, and bifurcations.

Another calculation method that is used is based on the Darcy-Weibach equation, which is presented in Equation 4.27:

$$\Delta p = K\frac{V^2}{2}\rho \tag{4.27}$$

The parameter K is equivalent to $f\frac{L}{D}$. This parameter is dimensionless and it illustrates the effect that each accessory has on the pressure loss. This parameter is highlighted by the manufacturer of the accessory and it varies with the type of material, length, and diameter of the accessory.

# Chapter 5

# Results

## 5.1 Hydrogen piping

### 5.1.1 Hydrogen compressor

AtlasCopco's proposed solution is a multistage compressor comprised of three hydraulic boosters with either one or two compression stages each, which receive 30 bar of hydrogen gas from the electrolyzer. Figure 5.1 is a representation of one of the boosters.

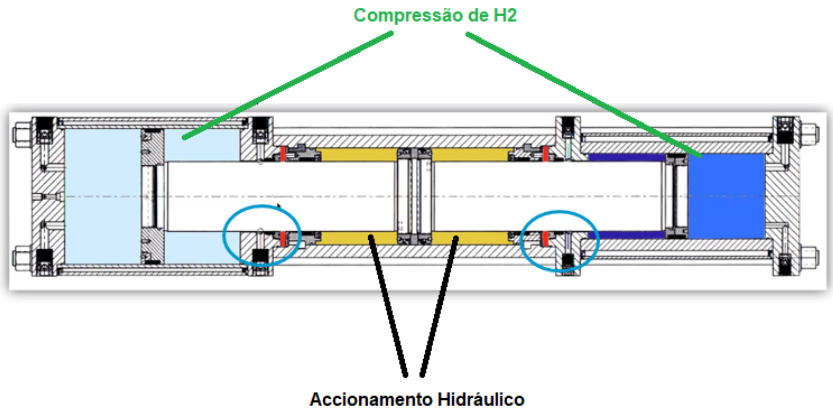



Figure 5.1: Booster example.

This hydrogen gas is then compressed until the desired output pressure of 1,000 bar is reached.

- Booster 1 (2 compression stage) from 30 to 185 bar, 55 $kW$.
- Booster 2 (1 compression stage) from 185 to 500 bar, 22 $kW$.
- Booster 3 (1 compression stage) from 500 to 1000 bar, 11 $kW$.

During compression, the temperature of the hydrogen gas increases to around 37 $°C$. The flow rate stated in the compressor's data sheet is 200 $Nm^3/h$. Note that the unit used by the supplier was $Nm^3/h$ and that refers to the volumetric flow rate at the pressure of 1 atm and 0 $°C$. This value

needs to be converted to mass flow rate, $\dot{m}_{1atm,0°C}$, (Equation 5.1), which is going to be constant throughout all the compression, and then converted back to volumetric flow rate, $Q_{1000bar}$, at the functioning pressure, 1000 bar (Equation 5.2). Knowing the value of hydrogen gas density at 1 atm and 0 $°C$ (0.0888 $kg/m^3$) and knowing the density at 1000 bar and 37 $°C$ (48 $kg/m^3$, as it can be taken from Appendix A) this calculation is possible:

$$\dot{m}_{1atm,0°C} = \rho_{1atm,0°C} \cdot Q \tag{5.1}$$

$$Q_{1000bar} = \frac{\dot{m}_{1atm,0°C}}{\rho_{1000bar}} \tag{5.2}$$

The value for the volumetric flow rate at the functioning pressure is 0.422 $m^3/h$

This flow rate value implies that, in the best case, the filling process of the tanks will take, 99 minutes for type 1 tanks, and 67 minutes for type 2 tanks.

Figure 5.2 represents the compressor unit comprised of the three boosters. These boosters are installed on a 9-meter-wide container, Figure 5.3, and cost around 500,000 euros. Since the boosters are oil-free equipment, the compression procedure will not impact the purity of the Hydrogen.

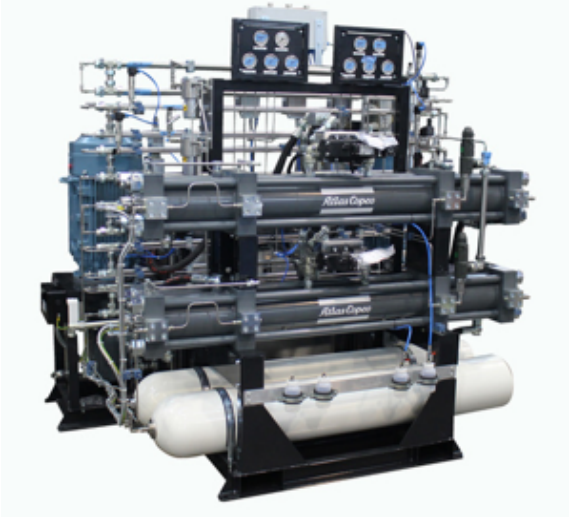


Figure 5.2: Compressor unit with the three boosters.

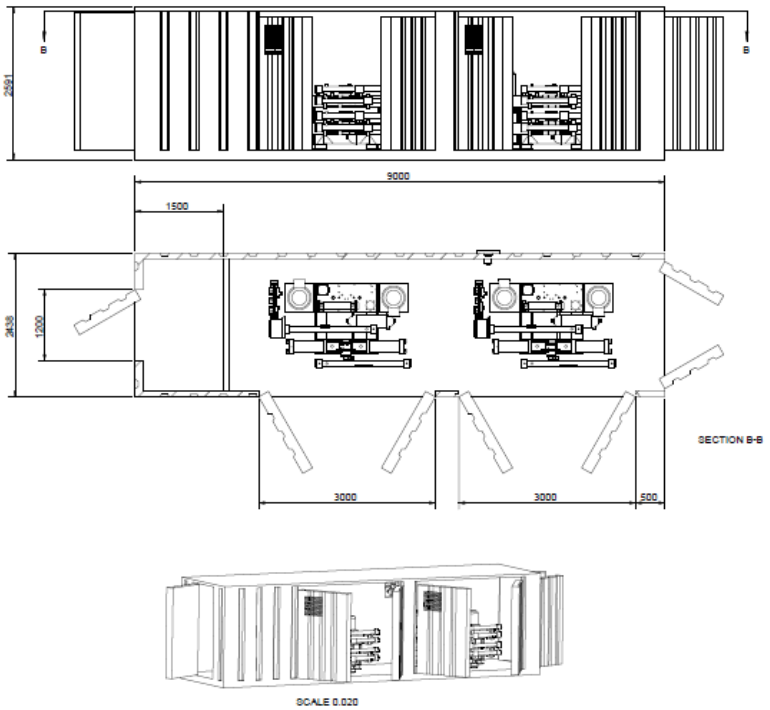



Figure 5.3: Illustration of the container with two compressor units.

Knowing the value of the power delivered to the boosters during compression, it is possible to calculate the amount of energy required to compress 1 kilogram of hydrogen gas, Equation 5.3.

$$E_{compression1kg} = \frac{Pot_{Total}}{\dot{m}} \tag{5.3}$$

The energy spent compressing 1 kg of hydrogen gas is 17837.83 $kJ$. Note that this value of consumed energy does not take into count the mechanical and volumetric efficiencies of the motor and the boosters, respectively.

When this value is compared to the GED of hydrogen which is 34 $kWh$ it can be concluded that the energy spent in compressing 1 kg of hydrogen is about 14% of the potential energy that can be extracted from the compressed gas.

This value can be raised when taking to account the electrolyzer energy consumption per kg of hydrogen produced, and the above-mentioned efficiencies.

### 5.1.2 Piping design

#### 5.1.2.1 Material

316L Stainless Steel was selected for the hydrogen pipeline due to its superior mechanical qualities and dependable corrosion resistance. In addition to being the standard steel for hydrogen applications because it resists hydrogen embrittlement, this material is widely available in a variety of profiles and sizes. The mechanical properties of this steel are presented in Appendix B.

#### 5.1.2.2 Inner and Outer diameter

Using the thick cylinder analysis methods described in the preceding chapter, the inner and outer diameter values satisfying both the Tresca and Von-Mises criteria are presented in Table 5.1.

Table 5.1: Maximum inner diameter (and thickness) that satisfy the Tresca and Von Mises Criteria

| Dout [mm] | Dinmax [mm] | tmax [mm] |
|---|---|---|
| 25 | 17.21 | 3.90 |
| 24 | 16.52 | 3.74 |
| 23 | 15.83 | 3.59 |
| 22 | 15.14 | 3.43 |
| 21 | 14.45 | 3.27 |
| 20 | 13.76 | 3.12 |
| 19 | 13.08 | 2.96 |
| 18 | 12.39 | 2.81 |
| 17 | 11.70 | 2.65 |
| 16 | 11.01 | 2.49 |
| 15 | 10.32 | 2.34 |
| 14 | 9.64 | 2.18 |
| 13 | 8.95 | 2.03 |
| 12 | 8.26 | 1.87 |
| 11 | 7.57 | 1.71 |
| 10 | 6.88 | 1.56 |

Due to limits surrounding the profile supplier (Appendix C) and valves (as it is going to be shown in section 5.1.3.2 and in the Appendix D), the values of the inner and exterior diameters of the pipeline were filtered, and the results are shown in Table 5.2.

Table 5.2: Possible outside diameters and corresponding maximum inside diameters of the pipeline

| Valve pipe tubing outside diameter [mm] | Maximum pipe inside diameter [mm] |
|---|---|
| 25 | 17 |
| 19 | 13 |
| 13 | 8 |

### 5.1.3 Pressure loss

#### 5.1.3.1 Straight line pressure loss

According to the pipe diameters presented in the preceding section, and assuming the roughness of stainless steel to be 1 $\mu$m and the viscosity of hydrogen to be 0.0000088 Pa.s, pressure loss

values for pipe lengths ranging from 0 to 5 meters were determined and are shown in Table 5.3. For all the diameters that were used in the calculation, the Reynolds number was always above 4000, which means that the flow was always turbulent.

Table 5.3: Pressure loss values (Pa) depending on pipeline length and interior diameter

| L [m] | Dint [mm] | | |
|---|---|---|---|
| | 17 | 13 | 8 |
| 0.0 | 0.0 | 0.0 | 0.0 |
| 0.1 | 0.7 | 2.6 | 27.3 |
| 0.2 | 1.5 | 5.2 | 54.6 |
| 0.3 | 2.2 | 7.9 | 81.9 |
| 0.4 | 2.9 | 10.5 | 109.1 |
| 0.5 | 3.6 | 13.1 | 136.4 |
| 0.6 | 4.4 | 15.7 | 163.7 |
| 0.7 | 5.1 | 18.4 | 191.0 |
| 0.8 | 5.8 | 21.0 | 218.3 |
| 0.9 | 6.5 | 23.6 | 245.6 |
| 1.0 | 7.3 | 26.2 | 272.9 |
| 1.1 | 8.0 | 28.9 | 300.1 |
| 1.2 | 8.7 | 31.5 | 327.4 |
| 1.3 | 9.4 | 34.1 | 354.7 |
| 1.4 | 10.2 | 36.7 | 382.0 |
| 1.5 | 10.9 | 39.4 | 409.3 |
| 1.6 | 11.6 | 42.0 | 436.6 |
| 1.7 | 12.3 | 44.6 | 463.8 |
| 1.8 | 13.1 | 47.2 | 491.1 |
| 1.9 | 13.8 | 49.9 | 518.4 |
| 2.0 | 14.5 | 52.5 | 545.7 |
| 2.1 | 15.2 | 55.1 | 573.0 |
| 2.2 | 16.0 | 57.7 | 600.3 |
| 2.3 | 16.7 | 60.4 | 627.6 |
| 2.4 | 17.4 | 63.0 | 654.8 |
| 2.5 | 18.1 | 65.6 | 682.1 |
| 2.6 | 18.9 | 68.2 | 709.4 |
| 2.7 | 19.6 | 70.9 | 736.7 |
| 2.8 | 20.3 | 73.5 | 764.0 |
| 2.9 | 21.0 | 76.1 | 791.3 |
| 3.0 | 21.8 | 78.7 | 818.6 |
| 3.1 | 22.5 | 81.4 | 845.8 |
| 3.2 | 23.2 | 84.0 | 873.1 |

Table 5.3: Pressure loss values (Pa) depending on pipeline length and interior diameter

| L [m] | Dint [mm] | | |
|---|---|---|---|
| | 17 | 13 | 8 |
| 3.3 | 23.9 | 86.6 | 900.4 |
| 3.4 | 24.7 | 89.2 | 927.7 |
| 3.5 | 25.4 | 91.9 | 955.0 |
| 3.6 | 26.1 | 94.5 | 982.3 |
| 3.7 | 26.8 | 97.1 | 1009.5 |
| 3.8 | 27.6 | 99.7 | 1036.8 |
| 3.9 | 28.3 | 102.4 | 1064.1 |
| 4.0 | 29.0 | 105.0 | 1091.4 |
| 4.1 | 29.7 | 107.6 | 1118.7 |
| 4.2 | 30.5 | 110.2 | 1146.0 |
| 4.3 | 31.2 | 112.9 | 1173.3 |
| 4.4 | 31.9 | 115.5 | 1200.5 |
| 4.5 | 32.6 | 118.1 | 1227.8 |
| 4.6 | 33.4 | 120.7 | 1255.1 |
| 4.7 | 34.1 | 123.4 | 1282.4 |
| 4.8 | 34.8 | 126.0 | 1309.7 |
| 4.9 | 35.5 | 128.6 | 1337.0 |
| 5.0 | 36.3 | 131.2 | 1364.3 |

#### 5.1.3.2 Valves and Local pressure loss

In the simplified schematic represented in Figure 5.4 a check valve is required after the H2 compressor (since it is very costly, must be safeguarded from overpressure by the implementation of safety measures).

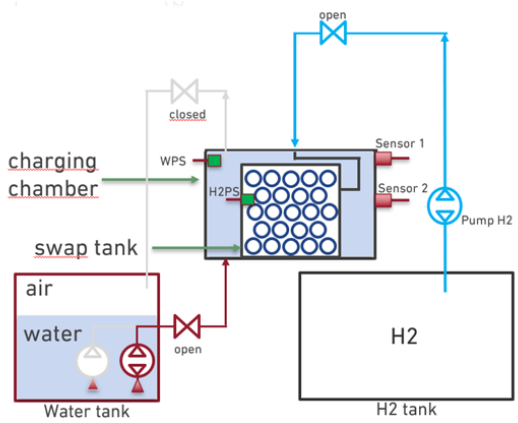



Figure 5.4: Proposed second water charging technique

The Retention/Check valve was selected to secure the hydrogen compressor, while the Globe valve was chosen to regulate the pipe flow. For the following pressure loss estimate, elbows were also accounted for, since they are a kind of equipment that would be utilized extensively in this application.

In conclusion, the pipeline must have the configuration indicated in Figure 5.5.

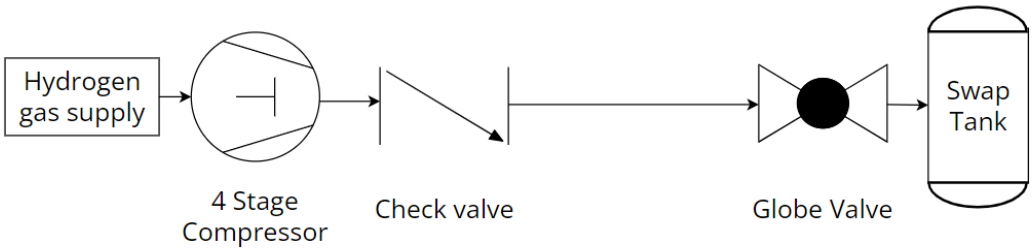



Figure 5.5: Proposed piping system configuration.

The flow regulating valve must be manufactured and operated in accordance with the above-described filling procedure. The valve must remain open until the pressure difference is zero and must then shut-in order for the hydrogen to mix and fill the swap tank's spheres evenly. For the proper working of the charging process, it is necessary to choose an actuator for this valve since the duration at which the pressure difference reaches zero might be extremely brief and it is impractical to do it manually.

The K values for the local pressure loss were acquired from Figure D.1 in Appendix D. Given the diameters specified in section 5.1.2.2 and the average flow velocity, it is possible to do the calculation stated in equation 4.27, the Darcy-Weibach equation. The pressure loss findings are presented in Table 5.4.

Table 5.4: Local pressure loss in different equipment

| Equipment | Dout [mm] | Din [mm] | K | V [m/s] | p [Pa] | p [bar] |
|---|---|---|---|---|---|---|
| Check Valve | 25 | 17 | 3.2 | 0.52 | 18.00 | 0.0018 |
| | 19 | 13 | 2.4 | 0.88 | 39.47 | 0.0039 |
| | 13 | 8 | 1.6 | 2.34 | 183.48 | 0.0183 |
| Globe Valve | 25 | 17 | 8.2 | 0.52 | 46.11 | 0.0046 |
| | 19 | 13 | 6.7 | 0.88 | 110.19 | 0.0110 |
| | 13 | 8 | 4.9 | 2.34 | 561.90 | 0.0562 |
| Medium Elbow (90 degrees) | 25 | 17 | 0.7 | 0.52 | 3.94 | 0.0004 |
| | 19 | 13 | 0.6 | 0.88 | 9.87 | 0.0010 |
| | 13 | 8 | 0.4 | 2.34 | 45.87 | 0.0046 |

## 5.2 Compressed air usage

For the air solutions described in the problem description section, the availability of ultra-high-pressure air compressors was investigated, and it was determined that there are no compressors that deliver the required pressures for these applications. Typical compressed air applications require discharge pressures between tenths or hundreds of bar. As a result, the investigation and implementation of compressed air solutions were not conducted.

## 5.3 Results Analysis

In this section it will be summarized the results found on the previous subsections. The chosen 4-stage compressor releases hydrogen gas at 1000 bar into the pipeline at 37 $°C$ at the volumetric flow rate of 0.422 $m^3/h$. Tank 1 type has a volume of 699.84 $l$ and the tank 2 type 472 $l$. With this flow rate the tanks charging times are 99 and 67 minutes for tanks 1 and 2, respectively.

For each kilogram of hydrogen gas that is compressed 17837.83 $kJ$ of energy is spent. Comparing that value to the hydrogen's GED, the value of potential energy per kg of hydrogen, it can be understood that in the best conditions, not considering the mechanical and volumetric efficiencies, 14% of hydrogen's potencial energy is lost in the compression process.

The material chosen for the hydrogen piping was the 316L stainless steel due to its good mechanical properties and high resistance to corrosion (fundamentally hydrogen embrittlement). The possible and suggested outside and inside diameters for the pipelines were 25/17, 19/13 and 13/8 milimiters. These values were obtained through thick cylinder analysis and complying to the Von-Mises and Tresca criteria.

For these possible outcomes, the pressure loss in a straight line was calculated and for 5 meters of pipeline the following results were obtained. For the internal diameter of 17 $mm$, 36 $Pa$ of pressure is lost, for 13 $mm$, 131 $Pa$, and for 8 $mm$, 1364 $Pa$.

The valves chosen for the correct control and security of the piping system and its components were a check valve and a flow regulating globe valve. It was presented the values of pressure loss for both the check valve and the globe valve depending on the different diameters at study. It was concluded that for the worst conditions the check valve provokes a loss of 183 $Pa$, and the globe valve 562 $Pa$, this happens when the interior diameter is 8 $mm$.

When considering a 25 $mm$ outside diameter and 17 $mm$ inside diameter hydrogen piping, one check valve, 5 meters of pipeline, one globe valve, and one elbow, there is pressure loss of 104 $Pa$. For the worst scenario, considering a 13 $mm$ outside diameter and 8 $mm$ inside diameter hydrogen piping, one check valve, 5 meters of pipeline, one globe valve, and one elbow, there is pressure loss of 2156 $Pa$.

Concluding, the pressure loss when using piping with 8 mm of interior diameter is roughly 20 times greater when compared to the pressure loss when using piping with 17 mm of interior diameter.

# Chapter 6

# Conclusions and Future Work

## 6.1 Conclusions

Without a question, hydrogen is one of the most intriguing fuel sources. Its gravimetric energy density is very desired, but its volumetric energy density is what makes hydrogen such a challenging fuel source. The necessity to subject hydrogen to high pressures in order to store large quantities of it in small, restricted places makes this gas a costly and, above all, very hazardous alternative to the fossil fuels that are so prevalent today.

Due to its excellent mechanical properties and resistance to hydrogen embrittlement, 316L stainless steel was chosen for the piping system. Hydrogen embrittlement is a phenomenon that causes many structural problems, such as cracks, and prevents carbon-based materials from being used in hydrogen applications.

The selected compressor unit, comprised of three boosters and four compression stages, discharges hydrogen gas at 1000 pressure and about 37 $°C$. With this information, it was able to determine that this compression unit fills the proposed tanks in 99 minutes for the tank with a capacity of 699 $l$, tank type 1, and in 67 minutes for the tank with a capacity of 472 $l$, tank type 2. These intervals are advantageous if the tanks are released from the charging station at a slower pace than they are charged. Due to the duration of these charging periods, the empty tanks coming from the vehicles must be replaced. The charging station should have several charged backup tanks ready for installation.

In addition, it was possible to discover that, for this compression unit, the minimum energy consumed during the compression process accounts for about 14% of the hydrogen gas GED. Since this calculated energy value does not include any mechanical or volumetric efficiencies of the compression unit, the energy consumption of the electrolyzer, or the energy required to compress the water that must be positioned around the swap tank, it can be concluded that significant energy losses are expected in this process.

The pressure loss in the hydrogen pipeline was calculated, and it was possible to conclude that for pipelines with interior diameters ranging from 17 to 8 millimeters, a length of 5 meters, and valves required for the proper safety of the pipeline and flow control, the best value for pressure

loss was for the largest interior diameter, which was 17 millimeters. This final result was 104 *Pa*, the worst-case scenario was for the smallest diameter evaluated, 8 *mm*, and the pressure loss was around 2156 *Pa*, which is approximately 20 times greater than the prior estimate.

After the completion of this research, it was able to determine that despite hydrogen's favorable properties as a fuel vector, such as minimal pollutant emissions and high gravimetric density, it still poses certain difficulties when implementing the systems necessary to make hydrogen a fuel source. The majority of carbon-based materials cannot be used in hydrogen applications, and a significant amount of energy is expended compressing hydrogen gas into fuel cells of the proper size for transportation/mobility applications. And despite the fact that a significant amount of research is being performed to make hydrogen gas a safer fuel source, the gas's properties continue to present a number of difficulties, particularly when it comes into contact with atmospheric air.

## 6.2 Future Work

Since there was no time to further investigate the feasibility of the implementation of the pressurized water outside of the swap tank, it would be of big importance to study what are the requirements to materialize the pressurizing system for water.

It would also be important to study the situation where there are variations in temperature for the spheres charging process. It was assumed that this process was done at a constant temperature since there was water outside the swap tank, so the heat flux would be directed outside the swap tank.

The materials and components for the water piping system, as well as the dimensioning of the charging chamber that needs to shelter the swap tanks, regardless of the different dimensions that they may have, should also be investigated.

A further assessment of the hydrogen piping system should be done in order to recognize if the piping system complies with standards and codes, either presented by the American Society of Mechanical Engineers (ASME), American National Standards Institute (ANSI), International Organization for Standardization (ISO), and Deutsches Institut für Normung (DIN).

# Bibliography


[1] Gianluca Valenti. Hydrogen liquefaction and liquid hydrogen storage. In *Compendium of hydrogen energy*, pages 27–51. Elsevier, 2016.

[2] Colleen Spiegel. *Designing and building fuel cells*, volume 87. Mcgraw-hill New York, 2007.

[3] Gustavo Pinto, Joaquim Monteiro, A. Baptista, Leonardo Ribeiro, and José Leite. Study of the permeation flowrate of an innovative way to store hydrogen in vehicles. *Energies*, 14:6299, 10 2021.

[4] James Larminie, Andrew Dicks, and Maurice S McDonald. *Fuel cell systems explained*, volume 2. J. Wiley Chichester, UK, 2003.

[5] A. Baptista, Carlos Pinho, Gustavo Pinto, Leonardo Ribeiro, Joaquim Monteiro, and Tiago Santos. Assessment of an innovative way to store hydrogen in vehicles. *Energies*, 12:1762, 05 2019.

[6] Lars G Stenmark. Hydrogen effects on silicon microsystems. 2009.

[7] Lars G Stenmark. High pressure hydrogen storage. 2009.

[8] Tiago Santos. Estudo de um sistema de armazenamento de hidrogénio para veículos. Unpublished paper, 2018.

[9] EIGA European Industrial Gases Association. *HYDROGEN TRANSPORTATION PIPELINES*. 2014.

[10] Evangelos Tzimas, C Filiou, SD Peteves, and JB Veyret. Hydrogen storage: state-of-the-art and future perspective. *EU Commission, JRC Petten, EUR 20995EN*, 2003.

[11] HiP High Pressure Equipment. *Valves, Fittings Tubing, Pressure Vessels Reactors*. 2020.

[12] Brian Nesbitt. *Handbook of valves and actuators: valves manual international*. Elsevier, 2011.

[13] Paulo M S Tavares de Castro. *Tensões em Peças Cilíndricas*. DEMec, Faculdade de Enegenharia da Universidade do Porto, 2019.

[14] V Féodossiev. Résistance des matériaux. 01 1976.

[15] Stephen Timoshenko. Resistance des materiaux. *Paris: Dunod, |c1968/1972*, -1, 01 1968.

[16] Vincenzo Vullo. Circular cylinders and pressure vessels. 3, 01 2014.

[17] Carlos Manuel Coutinho Tavares de Pinho. *Sistemas Térmicos*. DEMec, Faculdade de Enegenharia da Universidade do Porto, 2016.

[18] Bruce Roy Munson, Theodore Hisao Okiishi, Wade W Huebsch, and Alric P Rothmayer. *Fluid mechanics*. Wiley Singapore, 2013.

[19] John R Backhurst and John H Harker. *Tecnologia Química, vol. IV*. Fundação Calouste Gulbenkian.

# Appendix A

# Hydrogen Density

*Hydrogen Analysis Resource Center:* ***Hydrogen Density ($kg/m^3$) at Different Temperatures ($^\circ C$) and Pressures (MPa)***

| Temperature (°C) | Pressure (MPa) | | | | | | |
|---|---|---|---|---|---|---|---|
| | 0.1 | 1 | 5 | 10 | 30 | 50 | 100 |
| -255 | 73.284 | 74.252 | | | | | |
| -250 | 1.1212 | 68.747 | 73.672 | | | | |
| -225 | 0.5081 | 5.5430 | 36.621 | 54.812 | 75.287 | | |
| -200 | 0.3321 | 3.3817 | 17.662 | 33.380 | 62.118 | 74.261 | |
| -175 | 0.2471 | 2.4760 | 12.298 | 23.483 | 51.204 | 65.036 | |
| -150 | 0.1968 | 1.9617 | 9.5952 | 18.355 | 43.079 | 57.343 | |
| -125 | 0.1636 | 1.6271 | 7.9181 | 15.179 | 37.109 | 51.090 | 71.606 |
| -100 | 0.1399 | 1.3911 | 6.7608 | 12.992 | 32.614 | 46.013 | 66.660 |
| -75 | 0.1223 | 1.2154 | 5.9085 | 11.382 | 29.124 | 41.848 | 62.322 |
| -50 | 0.1086 | 1.0793 | 5.2521 | 10.141 | 26.336 | 38.384 | 58.503 |
| -25 | 0.0976 | 0.9708 | 4.7297 | 9.1526 | 24.055 | 35.464 | 55.123 |
| 0 | 0.0887 | 0.8822 | 4.3036 | 8.3447 | 22.151 | 32.968 | 52.115 |
| 25 | 0.0813 | 0.8085 | 3.9490 | 7.6711 | 20.537 | 30.811 | 49.424 |
| 50 | 0.0750 | 0.7461 | 3.6490 | 7.1003 | 19.149 | 28.928 | 47.001 |
| 75 | 0.0696 | 0.6928 | 3.3918 | 6.6100 | 17.943 | 27.268 | 44.810 |
| 100 | 0.0649 | 0.6465 | 3.1688 | 6.1840 | 16.883 | 25.793 | 42.819 |
| 125 | 0.0609 | 0.6061 | 2.9736 | 5.8104 | 15.944 | 24.474 | 41.001 |

Source:
NIST Reference Fluid Thermodynamic and Transport Properties Database (REFPROP): Version 8.0
http://www.nist.gov/srd/nist23.htm

Figure A.1: Hydrogen density values at different temperatures and pressures.

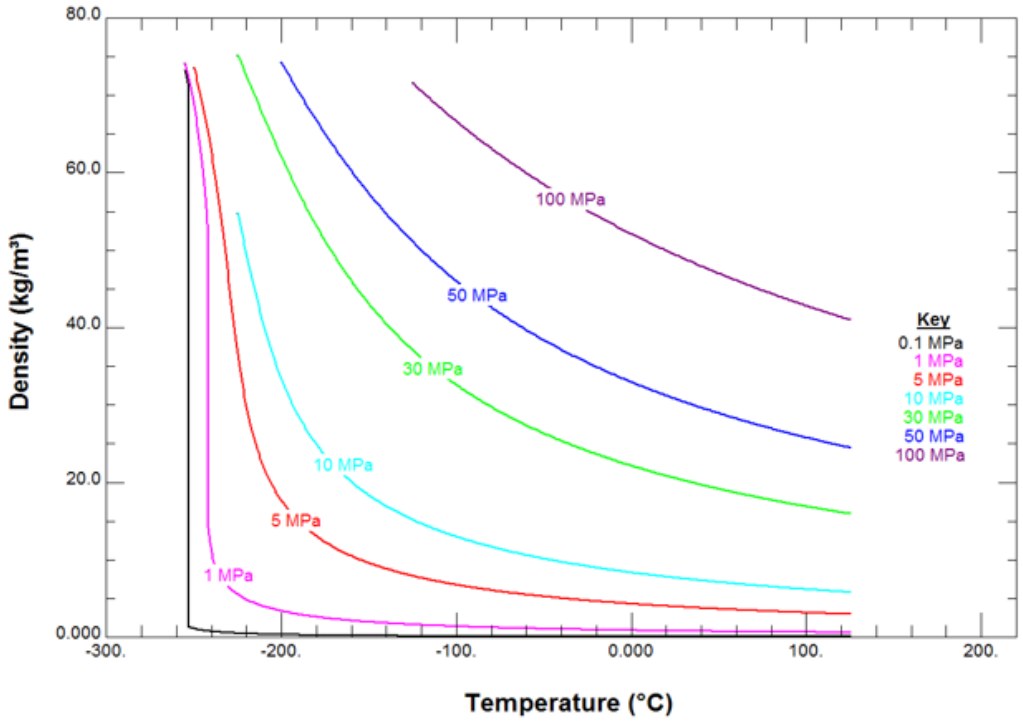



Figure A.2: Hydrogen density variation at different temperatures and pressures.

The value taken for the hydrogen density for 1000 bar (100 MPa) and 37 $°C$ was rounded to 48 $kg/m^3$. Values provided by NIST Reference Fluid Thermodynamic and Transport Properties Database.

# Appendix B

# 316L Stainless Steel properties

**COMPOSIÇÃO QUÍMICA (%):**

| C | Si | Mn | Ni | Mo | Cr |
|---|---|---|---|---|---|
| ≤ 0,07 | ≤ 1,00 | ≤ 2,00 | 10,00 - 13,00 | 2,00 - 2,50 | 16,50 - 18,50 |

Figure B.1: 316L stainless steel chemical composition.

**PROPRIEDADES:**

Densidade: 8,00 Kg/dm³

Coeficiente de Dilatação Térmica, $10^{-6}$m/mK:

| 20 a 600 °C | 20 a 500 °C | 20 a 400 °C | 20 a 300 °C | 20 a 200 °C | 20 a 100 °C |
|---|---|---|---|---|---|
| --- | 18,0 | 17,5 | 17,0 | 16,5 | 16,0 |

Condutibilidade Térmica, W/mK:

| 400 °C | 200 °C | 20 °C |
|---|---|---|
| --- | --- | 15 |

Módulo de Elasticidade, GPa:

| 600 °C | 500 °C | 400 °C | 300 °C | 200 °C | 100 °C | 20 °C | 0 °C | -100 °C |
|---|---|---|---|---|---|---|---|---|
| --- | 165 | 172 | 179 | 186 | 194 | 200 | --- | --- |

Figure B.2: 316L stainless steel properties.

| Propriedades Mecânicas: | | | | |
|---|---|---|---|---|
| ∅ (mm) | **Espessura (t)** (mm) | **Rm** (MPa) | **Rp0,2** (MPa) | **A%** (L0=5do) |
| ≤ 10 | ≤ 10 | 600 – 950 | ≥ 400 | ≥ 25 |
| ≤ 16 | ≤ 16 | 580 – 950 | ≥ 380 | ≥ 25 |
| ≤ 40 | ≤ 40 | 500 – 850 | ≥ 200 | ≥ 30 |
| ≤ 63 | ≤ 63 | 500 – 850 | ≥ 200 | ≥ 30 |

Figure B.3: 316L stainless steel mechanical properties.

These properties were provided by the company Ramada Aços®.

# Appendix C

# Steel tube profile specifications

**Detail Description**

| | |
|---|---|
| Commodity | Stainless Steel Pipe/Tube |
| Material Grade | 300 series |
| Type | seamless and welding pipe/tube |
| Shape | Round pipe, Square pipe, Rectangular pipe |
| Surface | Pickling/Polished/Satin/Hairline/Mirror Finish |
| Outside diameter | 6mm-630mm(seamless pipe)9.5mm-1200mm(welding pipe)or as customer's requirement |
| Wall thickness | 2.5mm-30mm(seamless pipe)0.3-40mm(welded pipe)or as customer's requirement |
| Length | 6 Meters and as customer's requirement |
| End Type | Plain endButt weld endBeveled end |
| Standards | AISI ASTM JIS SUS and GB |
| Certifications | ISO 9001,SGS,BV |
| Packing | Seaworthy wooden pallet or according to client's requirement |
| MIQ | 1 ton or free samples |
| Price term | FOB China port & CIF Destination Port & CFR |
| Advantage | Showing the splendor of your quality ; Strong corrosion resistance and decorative effect ; Durable and beautiful in good taste . |

Figure C.1: 316L stainless steel profile information.

This information is publicly displayed in HONGTU's website, the supplier chosen for the tube profile of the hydrogen piping system.

# Appendix D

# K values of different accessories

| | | Cotovelo 90° raio | | | | Curva | | | Entrada | | Saida | Válvula | | | Tê | | |
|---|---|---|---|---|---|---|---|---|---|---|---|---|---|---|---|---|---|
| | | 90° | | | 45° | 90° | | 45° | Normal | Borda | | Guilhotina /Cunha | Globo | Retenção | Saida | | |
| | | longo | médio | curto | | R/D=1 ½ | R/D=1 | | | | | | | | direita | lado | bilateral |
| Diâmetro (D) | |  |  |  |  |  |  |  |  |  |  |  |  |  |  |  |  |
| mm | in | | | | | | | | | | | | | | | | |
| 13 | ½ | 0,3 | 0,4 | 0,5 | 0,2 | 0,2 | 0,3 | 0,2 | 0,2 | 0,4 | 0,4 | 0,1 | 4,9 | 1,6 | 0,3 | 1,0 | 1,0 |
| 19 | ¾ | 0,4 | 0,6 | 0,7 | 0,3 | 0,3 | 0,4 | 0,2 | 0,2 | 0,5 | 0,5 | 0,1 | 6,7 | 2,4 | 0,4 | 1,4 | 1,4 |
| 25 | 1 | 0,5 | 0,7 | 0,8 | 0,4 | 0,3 | 0,5 | 0,2 | 0,3 | 0,7 | 0,7 | 0,2 | 8,2 | 3,2 | 0,5 | 1,7 | 1,7 |
| 32 | 1 ¼ | 0,7 | 0,9 | 1,1 | 0,5 | 0,4 | 0,6 | 0,3 | 0,4 | 0,9 | 0,9 | 0,2 | 11,3 | 4,0 | 0,7 | 2,3 | 2,3 |
| 38 | 1 ½ | 0,9 | 1,1 | 1,3 | 0,6 | 0,5 | 0,7 | 0,3 | 0,5 | 1,0 | 1,0 | 0,3 | 13,4 | 4,8 | 0, | 2,8 | 2,8 |
| 50 | 2 | 1,1 | 1,4 | 1,7 | 0,8 | 0,6 | 0,9 | 0,4 | 0,7 | 1,5 | 1,5 | 0,4 | 17,4 | 6,4 | 1,1 | 3,5 | 3,5 |
| 63 | 2 ½ | 1,3 | 1,7 | 2,0 | 0,9 | 0,8 | 1,0 | 0,5 | 0,9 | 1,9 | 1,9 | 0,4 | 21,0 | 8,1 | 1,3 | 4,3 | 4,3 |
| 75 | 3 | 1,6 | 2,1 | 2,5 | 1,2 | 1,0 | 1,3 | 0,6 | 1,1 | 2,2 | 2,2 | 0,5 | 26,0 | 9,7 | 1,6 | 5,2 | 5,2 |
| 100 | 4 | 2,1 | 2,8 | 3,4 | 1,5 | 1,3 | 1,6 | 0,7 | 1,6 | 3,2 | 3,2 | 0,7 | 34,0 | 12,9 | 2,1 | 6,7 | 6,7 |
| 125 | 5 | 2,7 | 3,7 | 4,2 | 1,9 | 1,6 | 2,3 | 0,9 | 2,0 | 4,0 | 4,0 | 0,9 | 43,0 | 16,1 | 2,7 | 8,4 | 8,4 |
| 150 | 6 | 3,4 | 4,3 | 4,9 | 2,3 | 1,9 | 2,5 | 1,1 | 2,5 | 5,0 | 5,0 | 1,1 | 51,0 | 19,3 | 3,4 | 10,0 | 10,0 |
| 200 | 8 | 4,3 | 5,5 | 6,4 | 3,0 | 2,4 | 3,3 | 1,5 | 3,5 | 6,0 | 6,0 | 1,4 | 67,0 | 25,0 | 4,3 | 13,0 | 13,0 |
| 250 | 10 | 5,5 | 6,7 | 7,9 | 3,8 | 3,0 | 4,2 | 1,8 | 4,5 | 7,5 | 7,5 | 1,7 | 85,0 | 32,0 | 5,5 | 16,0 | 16,0 |
| 300 | 12 | 6,1 | 7,9 | 9,5 | 4,6 | 3,6 | 4,8 | 2,2 | 5,5 | 9,0 | 9,0 | 2,1 | 102,0 | 38,0 | 6,1 | 19,0 | 19,0 |
| 350 | 14 | 7,3 | 9,5 | 10,5 | 5,3 | 4,4 | 5,4 | 2,5 | 6,2 | 11,0 | 11,0 | 2,4 | 120,0 | 45,0 | 7,3 | 22,0 | 22,0 |

Figure D.1: Accessories K values for local pressure calculation.[19]